8-2014

Carbon Cycling Dynamics Inferred from Carbon Isotope Sourcing in a Mid-Latitude Karst-Influenced River

Kegan N. McClanahan
Western Kentucky University, kegan.mcclanahan048@topper.wku.edu

CARBON CYCLING DYNAMICS INFERRED FROM CARBON ISOTOPE SOURCING IN A MID-LATITUDE KARST-INFLUENCED RIVER

A Thesis
Presented to
The Faculty of the Department of Geography and Geology
Western Kentucky University
Bowling Green, Kentucky

In Partial Fulfillment
of the Requirements for the Degree
Master of Science

By
Kegan N. McClanahan

August 2014

CARBON CYCLING DYNAMICS INFERRED FROM CARBON ISOTOPE SOURCING IN A MID-LATITUDE KARST INFLUENCED RIVER

Date Recommended 11 July 2014

Jason S. Polk, Director of Thesis

Chris Groves

Scott Grubbs

Dean, Graduate School

8-8-14
Date

ACKNOWLEDGEMENTS

Not just completing, but thriving in a graduate program is not a journey you take by yourself. Try as you might to make time for everyone and everything in your life while surviving the rigors of graduate school, you will not succeed. This lesson I learned the hard way. While my family is the most understanding group of people in my life, it was always hard to inform them I won't be coming to see them for some time. For their continued support, guidance, humor, patience and understanding, I am forever thankful.

I would not be writing this today if not for my thesis advisor, Jason Polk. We have shared both good memories and bad, long nights, fun days in the field, and everything in between during our two-year journey together. I am eternally grateful for your steadfast commitment to help me grow as an academic, a researcher, and as a person. Thank you.

My thesis would not have existed without the support and guidance of my committee members, Dr. Chris Groves and Dr. Scott Grubbs. Both of you have my eternal respect and admiration; I would not be where I am today without your help and support. Although not on my committee, Drs. Ouida and Albert Meier were instrumental in the Green River Project and have taught me a great deal. I am extremely grateful for the many discussions and excellent guidance on such a large and complicated undertaking. The Green River Preserve provided an outstanding field site and played a critical role in my data collection.

There are many people who have helped me along the way in one form or another and I am extremely grateful. I would like to thank Dan Nedvidek personally for spending multiple weekends helping to get the Green River project off the ground. We

have shared a lot of late nights together in the office, too many venting sessions to count, a few rounds at the bar, and one too many rounds of hall ball – thank you! I would not have survived my first semester of graduate school without the wisdom and guidance of Leslie North. You were a beacon of sanity in my chaotic first year and a world-class advisor on all matters of life - thank you! Dr. Suvankar Chakraborty was instrumental in making sense of my data and never will I meet a more respectable lab manager. To you, I owe a great deal of thanks. I would also like to thank Veronica Hall, Jeremy Simmons, Ellen Barringer, Jonathan Oglesby, and Caleb Koostra. You have been invaluable field assistants, lab assistants, and masters at making the world's finest riverine carbon cycle diagrams - thank you! Last, but not least, I would have spent many lonely days out in the field without the assistance of Laura Osterhoudt. Thank you for all the help you have given me over the past two years!

CONTENTS

LIST OF FIGURES

LIST OF TABLES

LIST OF EQUATIONS

CARBON CYCLING DYNAMICS INFERRED FROM CARBON ISOTOPE SOURCING IN A MID-LATITUDE KARST-INFLUENCED RIVER

Kegan McClanahan August 2014 73 Pages

Directed by: Jason S. Polk, Chris Groves, and Scott Grubbs

Department of Geography and Geology Western Kentucky University

As ever-increasing levels of carbon dioxide alter the chemistry of the Earth's atmosphere, understanding the global carbon cycle becomes increasingly important. A particularly important component is the riverine carbon cycle, as rivers are the primary conduits for dissolved inorganic carbon from terrestrial watersheds to ocean basins. Stable carbon isotopes ($^{13}C/^{12}C$) were collected weekly and input into the mixing model *IsoSource* to delineate seasonal carbon sourcing along two nested basins in the upper Green River System, Kentucky. In the more siliciclastic upstream catchment, dissolved inorganic carbon (DIC) was primarily derived from soil respiration (34%). Groundwater dissolving carbonate bedrock and carbonate dissolution/precipitation reactions contributed 31% and 11%, respectively. The more carbonate-dominated downstream catchment also was influenced greatly by soil respiration (35%). Due to the more pronounced levels of carbonate bedrock, carbonate reactions contributed double that of the upstream catchment (20%), with groundwater contributing 22%. Seasonally, the upstream basin gathered most DIC from soil respiration from late spring to winter. Early spring precipitation and still limited photosynthesis caused the primary carbon sourcing to shift to groundwater. Downstream, the primary source throughout the entire study period was soil respiration. Collectively, this study provides insight into the carbon cycling process in a mid-latitude, karstic river using carbon isotope sourcing to aid in the quantification of global carbon flux in the critical zone.

CHAPTER ONE: INTRODUCTION

1.1 Research Overview

Within the global discussion on climate change, atmospheric carbon dioxide (CO_2) is receiving increased attention due to its profound ability to impact global climate in addition to its inherent complex dynamics within natural systems. While occurring naturally, atmospheric carbon dioxide is increasing from anthropogenic activities, such as deforestation and burning of fossil fuels (Andres et al., 1999; Keeling et al., 1989; 2005; 2011). The debate continues regarding the extent to which anthropogenic activities influence global climate; however, there exists a growing body of evidence that supports the argument for anthropogenic emissions of greenhouse gases (carbon dioxide, methane, nitrous oxide) influencing natural climate cycles (Barnett et al., 2001; IPCC, 2007; Lean and Rind, 2008; Kininmonth, 2010). Atmospheric carbon dioxide is one reservoir in the vast global carbon cycle. The global carbon cycle contains numerous reservoirs and fluxes; two important fluxes to climate change are the interplay between the atmosphere and both fluvial and oceanic ecosystems.

The cycling of carbon dioxide between surface waters and the atmosphere is well studied in both oceanic ecosystems (Fan et al., 1998; Cox et al., 2000) and in fluvial systems (Fonselius et al., 1956; Rhode, 1990; Enting 1994; Zhang et al., 1995; Wigley et al., 1996; Finlay, 2003; del Giorgio and Williams, 2005; Doctor et al., 2008; Wooten and Tsokos, 2010; Keeling et al., 2011). Rivers represent the primary conduits of dissolved inorganic carbon (DIC) from terrestrial ecosystems to ocean basins (Striegl et al., 2012). The amalgamation of internal cycling and external inputs is displayed in the concentrations of DIC, in addition to other chemical constituents (Finlay, 2003; Szramek

and Walter, 2004). The riverine processes that influence total DIC flux are: (1) photosynthesis, (2) respiration, (3) water-air interchange of gases (CO_2), (4) groundwater inputs, and (5) geochemical reactions, including the precipitation/ dissolution of carbonate minerals (Redfield, 1958; Kling et al., 1992; Cox et al., 2000; Friedlingstein et al., 2001; Hope et al., 2001; Doctor et al., 2008).

Historically, the traditional methods involved in measuring the riverine carbon cycle strictly measured the concentrations of the organic and inorganic fractions (Degens et al., 1984). Recent studies show the combination of measuring concentrations with the addition of stable isotope analyses to be powerful in determining sources and sinks of carbon, internal cycling of carbon, and understanding the interactions between the river and the surrounding biosphere, hydrosphere, lithosphere, and atmosphere (Pawellek and Veizer, 1994; Flintop et al., 1996; Yang et al., 1996; Barth et al., 1998; Amiotte-Suchet et al., 1999; Aucour et al., 1999; Barth and Veizer, 1999; Telmer and Veizer, 1999; Pawellek et al., 2002; Barth et al., 2003; Das et al., 2005; Brunet et al., 2009; Tobias and Böhlke, 2011). Through the use of stable carbon isotopes ($^{13}C/^{12}C$), the sources, transformations, and fates of carbon within a river system can be identified.

The upper Green River in south-central Kentucky represents an important river in regards to regional biologic, geologic, hydrologic, and anthropogenic interests. Traversing a diverse range of landscapes including a karstified carbonate plateau, the upper Green River serves as the regional hydrologic base level; this region includes the world's longest known cave, the Mammoth Cave system. It is also the most biologically diverse river in the Ohio River system, with multiple endangered species (KGRCREP,

2010) and a high degree of primary productivity leading to a complex and dynamic ecosystem.

This investigation utilized a combination of high resolution geochemical and isotopic data to address seasonal carbon cycling along the upper Green River in south-central Kentucky. The combination of flux and sourcing information allowed the development of a mixing model to predict future changes in carbon cycling related to climate change. Using this approach, the study sought answers to the following questions:

- What are the sources of dissolved inorganic carbon in the karst influenced upper Green River?
- How do seasonal changes impact the inorganic carbon sourcing along the upper Green River?
- How does carbon sourcing vary between two nested basins; one, a more siliciclastic, less karstified catchment and the other a more carbonate, heavily karstified catchment?

Answering these questions helped to inform models and estimates of the global carbon cycle's terrestrial flux within a complex riverine system in a karst landscape.

1.2 Global Carbon Cycle

Carbon is cycled through both inorganic and organic fluxes between a network of reservoirs known as the carbon cycle (Fig. 1-1) (Post et al., 1990). While the three primary natural reservoirs with respect to natural interactions are the atmosphere, oceans, and terrestrial ecosystems, the largest amount of carbon exists in the bedrock as carbonate rock, oil and gas reserves, and coal beds. Of the three more active reservoirs,

the ocean constitutes the largest storage (Post et al., 1990). The smallest reservoir in terms of storage capacity is the atmosphere; however, due to the relatively short residence time of carbon in the atmosphere, it plays an important role (Post et al., 1990).

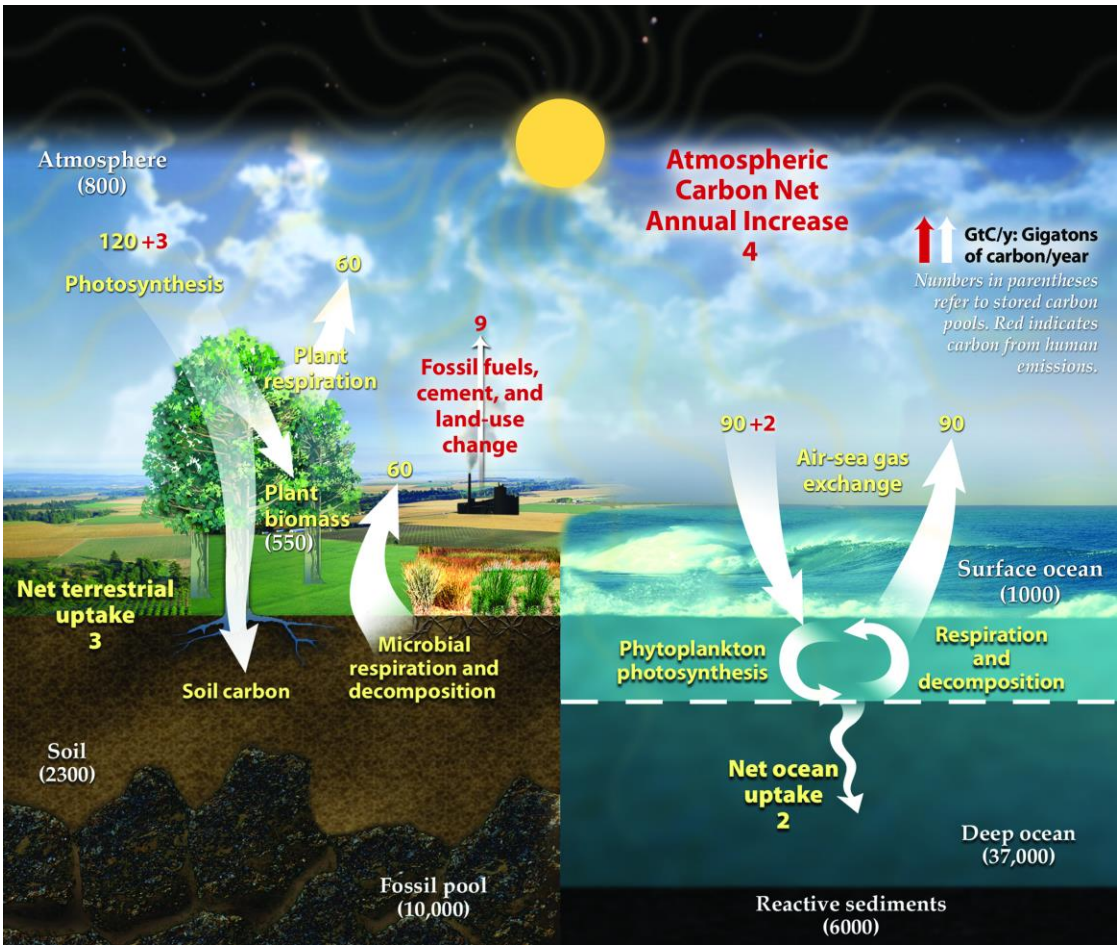

Fig. 1-1: Global carbon cycle. White numbers refer to estimates of natural reservoirs. The red numbers refer to estimates of human contributions to carbon reservoirs. The yellow numbers indicate fluxes between the reservoirs. Source: USDOE (2008).

The effects of carbon dioxide (CO_2) buildup in the atmosphere are well studied, with the primary effect being a direct relationship with increasing temperature. This causes a positive feedback loop on the greenhouse gas effect. As the Earth warms, the

effect of the positive feedback cycle is estimated to promote additional warming by approximately 16% over the span of a century (Cox et al., 2000; Scheffer et al., 2006). The positive feedback cycles that promote an increase in global temperatures are offset by negative feedback cycles that regulate global temperatures. Two of these negative feedback cycles are oceanic uptake of atmospheric CO_2 and vegetation/soil carbon in the terrestrial ecosystem (Friedlingstein et al., 2003).

While CO_2 emissions are buffered by absorption of atmospheric CO_2 by ocean waters and terrestrial ecosystems, this absorption is dependent on climate and the concentrations of greenhouse gases in the atmosphere. To understand the impact on global warming fully, these negative feedback cycles need to be explored further. According to Le Cléré et al. (2009) and Friedlingstein and Prentice (2010), an all-encompassing quantitative model of greenhouse gas emissions and absorption is required to plan for future greenhouse gas emissions and climate change.

One piece of the carbon cycle puzzle that needs further understanding is the effect of soil and vegetation on carbon uptake. Freidlingstein et al. (2003) reported the primary reason for differences between climate change cycles is the misunderstood role that soil and vegetation play in carbon uptake. Additionally, when looking at the global carbon cycle, there is a 30% gap between the expected and the measured total. This gap is known as the "missing carbon sink." More research is needed to quantify the effect of soil, vegetation, and carbonate bedrock uptake of carbon in the atmosphere (Esser et al., 2010; Davidson et al., 2010). Karst landscape development, controlled in part by soil and vegetation dynamics, provides an excellent opportunity to examine this relatively unknown piece of the carbon cycle (Crowther, 1983; Loàiciga et al., 2000).

1.3 Study Area

The Interior Low Plateaus physiographic region in the eastern United States hosts an extensive landscape of low-relief karst development (Fenneman, 1938; Palmer and Palmer, 2009). This physiographic region extends from the Appalachian Mountains in the east to the Mississippi River Valley in the west, and is bounded north-south by the Mississippi embayment and the southern extent of continental glaciation (the modern-day Ohio River). Within this region, the most well-developed karst landscapes of the United States are found (Palmer and Palmer, 2009).

Within the interior low plateaus, the upper Green River flows east to west draining 4,489 square kilometers of south-central Kentucky. The upper Green River flows from the headwaters over the Cincinnati Arch towards the Illinois Basin, where it transitions from a siliciclastic dominated landscape to one of highly karstified carbonates (Fig. 1-2). The upstream basin drains 1,919 km^2 over heterogeneous lithologies. Devonian shales (38%) and Mississippian limestones (51%) comprise the majority of the upstream basin's surficial geology. Select areas of the basin contain Ordovician dolostones (1.3%), Mississippian sandstones (1.1%), and younger Pleistocene and Holocene sands (6.4%) (Osterhoudt, 2014). The downstream basin includes the nested upstream basin, increasing the total drainage area to 4,489 km^2 (Osterhoudt, 2014). The downstream basin contains more homogeneous surficial lithologies. Surficially, the majority of the basin is composed of Mississippian carbonates (77%) that comprise the main Mammoth Cave-forming strata (Palmer and Palmer, 2009) (Fig. 1-3). Smaller areas include siliciclastic bedrock with shale (16.2%), sand (3.7%), sandstone (1.3%), and siltstone (0.2%) (Osterhoudt, 2014).

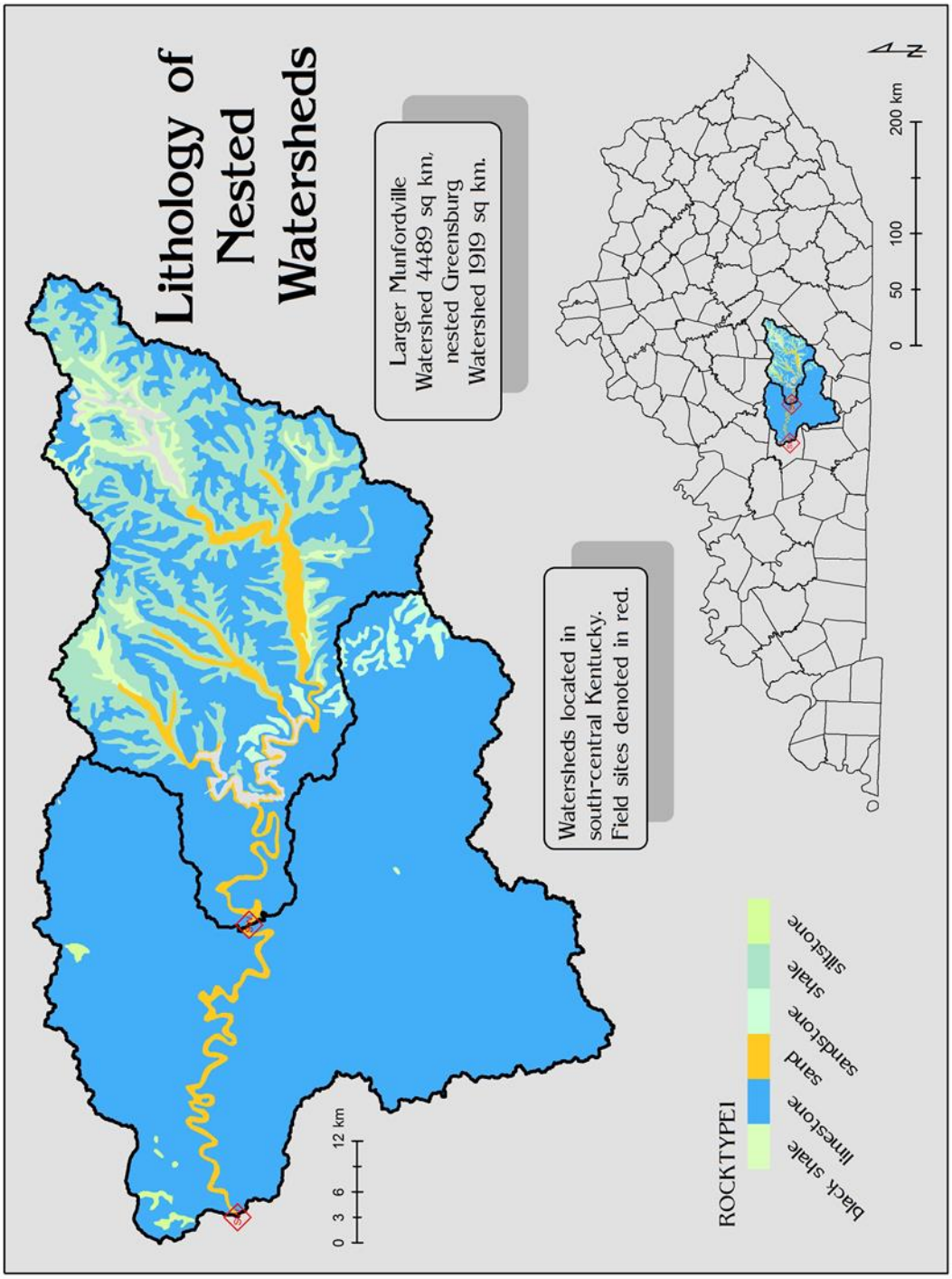

Fig. 1-2: Lithologies of the two nested watersheds. The field sites are denoted with red boxes. Source: Osterhoudt (2014).

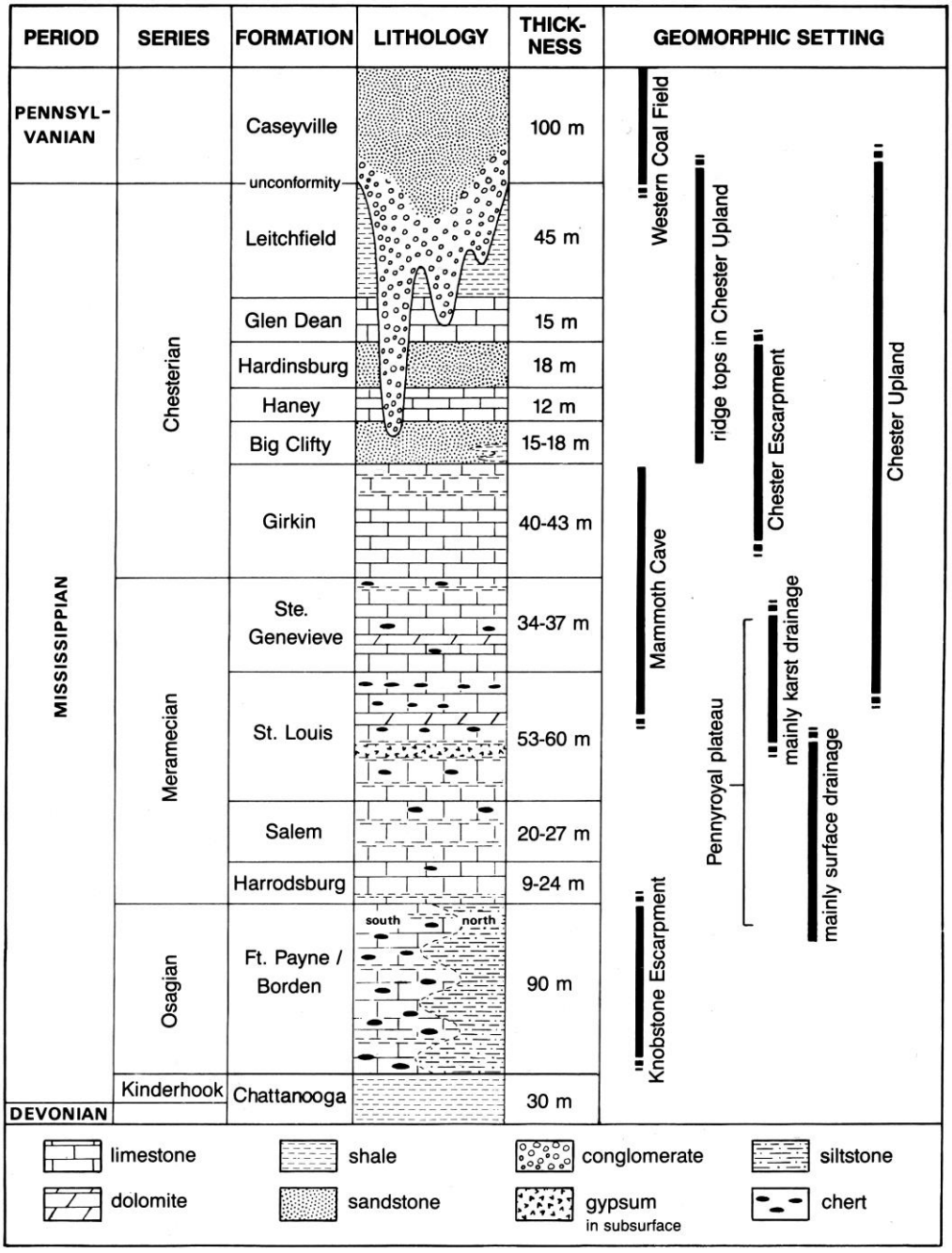

Fig. 1-3: Stratigraphic column showing the major bedrock formations in the region. Source: Palmer (1981).

Karst landscapes are dominated by chemical weathering of highly soluble bedrock leading to well-defined subsurface drainage networks via enlargement of secondary porosity (White, 1988; White and White, 1989; Quinlan et al., 1991; Ford and Williams, 2007; Palmer, 2007; Palmer and Palmer 2009). The majority of karst landscapes form on carbonate bedrock, primarily limestone and dolostone (Klimchouk et al., 2000). Carbonate bedrock landscapes represent one-fifth of the Earth's ice-free land surface and one quarter of all sedimentary rocks (Ford and Williams, 2007). Approximately 20-25% of the Earth's population is dependent on karst groundwater. These non-renewable environments represent important scientific, cultural, and economic regions of the world (Daoxian and Zaihua, 1998; Ford and Williams, 2007).

Weathering of bedrock, both siliciclastic and carbonate, plays an important role in the global carbon cycle. While siliciclastic bedrock dominates surface exposures, it is kinetically slower to weather compared to carbonate landscapes, which tend to dissolve faster, thus yielding their importance. In both landscapes, chemical weathering involves the respective removal and storage of atmospheric CO_2 in surface waters. Carbon dioxide readily dissolves into meteoric waters forming carbonic acid (H_2CO_3) with a pH of 5.66 when in equilibrium with atmospheric CO_2 (Drever, 1982). The water is furthered acidified as it infiltrates the soil column where plant root respiration and microbial activity produces up to two orders of magnitude more CO_2 than is currently present in the atmosphere (400 ppm). This acidic water is able to dissolve calcite through the following reaction (White and White, 1989; Drever, 1982):

$$2H_2O + CO_{2\,(atmospheric)} + CaCO_3 \leftrightarrow Ca^{2+} + 2HCO_3^- \qquad 1\text{-}1$$

By this equation, atmospheric carbon dioxide is transformed into bicarbonate (HCO_3^-) and stored in surface waters. Berner (1989) suggested that only over geologic timescales is the carbon sink effect generated by carbonate weathering balanced by a net production of carbon in the oceans, primarily through coral reef production

The upper Green River is the hydrologic base level for the region including Mammoth Cave, the world's longest mapped cave system. Several springs and tributaries flow into the Green River, including the Barren, Nolin, Pond, and Rough rivers (Benke and Cushing, 2005). Hess (1974) found there are over eighty springs along the Green River with the Goren Mill, Garvin, Blue South, Blue North, Mile 205.7, Dennison Ferry, Pike, Big, Ugly Creek, Floating Mill, Styx River, Echo River, Turnhole, Sal Hallow, Buffalo Creek, and Houchins Ferry springs all having finite flows that can be quantified. Hess (1974) also found that all runoff in the karstified region is discharged into the river via springs, and the majority of this discharge is through a select few large springs.

Within this physiographic region a temperate, humid climate persists with an average annual rainfall of 122 cm and an average temperature of 13.83°C between 1895 and 2005 (KCC, 2013). Hess and White (1988) found that precipitation deviates from the monthly average (1971-1973) by 60% in the summer compared to 40% in the winter. This coincides with the annual storm season in the summer months. The river response to the regional climate over the last 40 years produced an annually averaged discharge of 37,479 L/s (1,324 cfs) in Greensburg (Fig. 1-4) and an average of 82,098 L/s (2,899 cfs) in Munfordville (Fig. 1-5). During the time of record in Greensburg (1970-1974 and 2005-2007) the minimum and maximum discharges were 24,987 L/s (882 cfs) and

53,722 L/s (1,897 cfs), respectively. Munfordville records (1970-2013) show minimum and maximum discharges of 41,508 L/s (1,465 cfs) and 151,943 L/s (5,365 cfs), respectively (USGS, 2013).

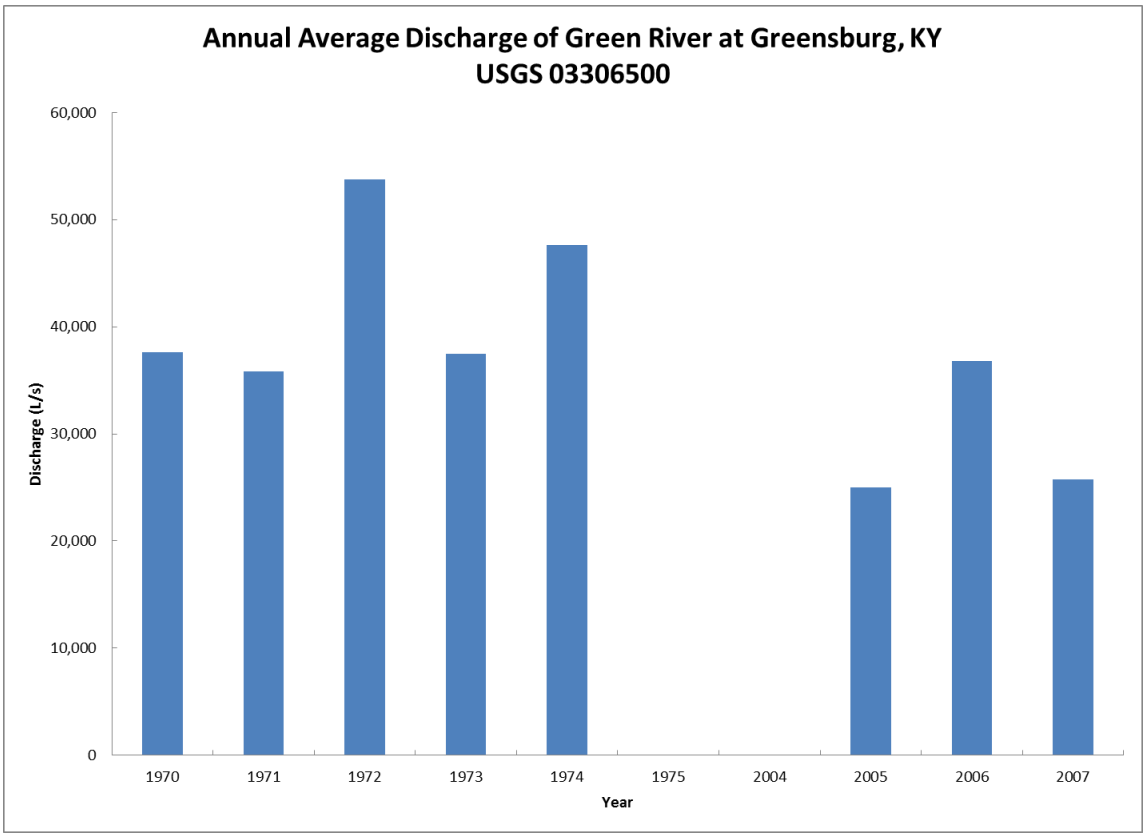

Figure 1-4: Yearly discharge averages for Greensburg (03306500) from 1970-1974 and 2005-2007. Source: USGS (2013).

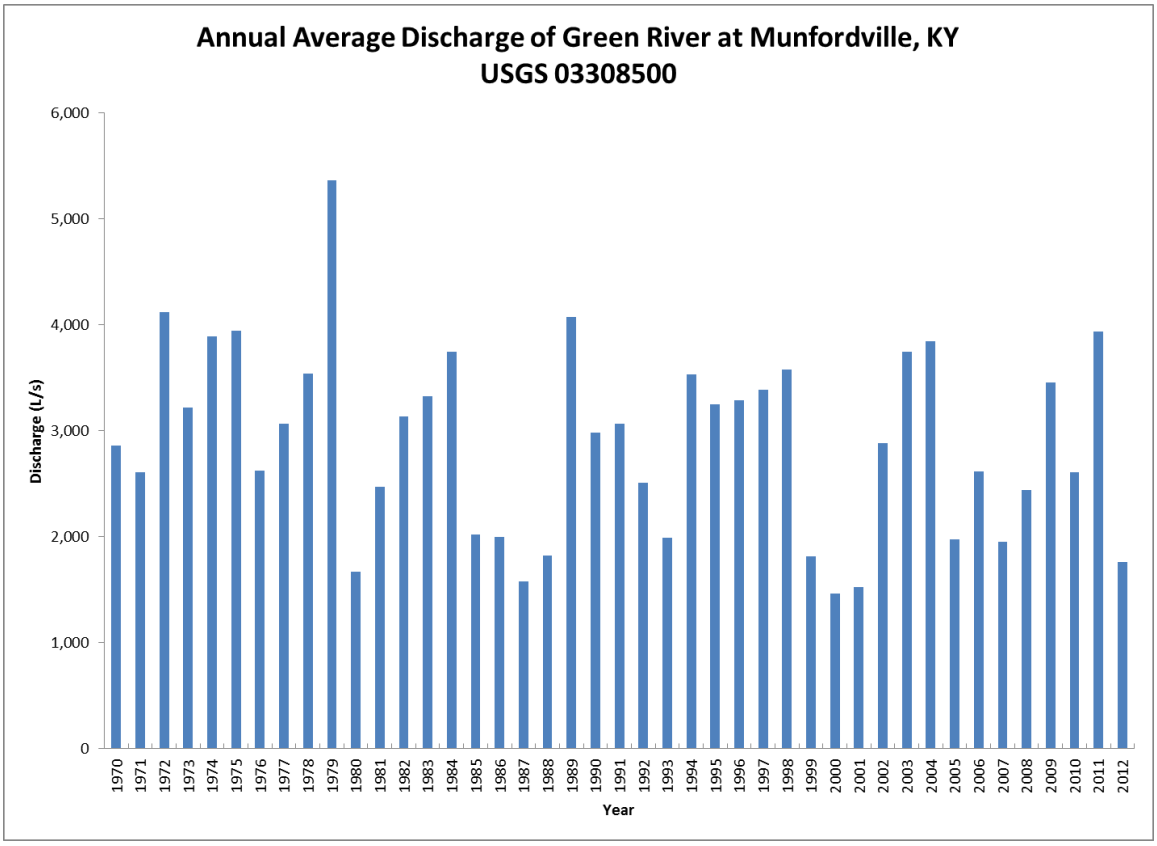

Fig. 1-5: Discharge averages for 1970 to 2012 for Munfordville, KY.
Source: USGS (2013) and author's calculations.

The Green River represents the most biologically diverse river within the Ohio River system (USACE, 2011). The study section, located between Greensburg and Munfordville, Kentucky, contains the greatest species diversity within the river. The U.S. Fish and Wildlife Service lists seven species within the Green River system as endangered (KGRCREP, 2010).

1.4 Stable Isotope Theory

Isotope geochemistry is used in research as environmental indicators, tracers, and as dating tools. Topics that isotopes have been and are still used for include food web

studies, nutrient flow, rock and mineral dating, paleoclimate and paleoenvironment reconstructions, weathering rates of geologic material, rock-water interactions, and material transport within reservoirs. Stable isotope geochemistry is based on the work of Murphy and Urey (1932), Nier and Gulbransen (1939), and Urey (1947; 1948).

Stable isotopes are measured as the ratio of the heavy isotope to the light isotope. Additionally, for each isotope system, the two most abundant isotopes are measured. When measuring isotopes, an apparent ratio, expressed as δ, of the isotopes is found and compared to a known standard, or reference (Eq. 1-2). The error is represented by (m).

$$\delta^{13}C_{sample} = \frac{m(^{13}C/^{12}C)_{sample} - m(^{13}C/^{12}C)_{reference}}{m(^{13}C/^{12}C)_{reference}} \qquad 1\text{-}2$$

Numerically, the differences in isotopic abundances are not significantly large, so to assist in determining concentration differences the values are multiplied by 1000 and reported in parts per thousand (per mil, ‰). The international reference standard for carbon stable isotopes is the Vienna Pee Dee Belemnite (VPDB). Using this notation, Equation 1.3 is expressed using the delta notation (δ) (Clark and Fritz, 1995):

$$\delta^{13}C_{sample} = \left(\frac{m(^{13}C/^{12}C)_{sample}}{m(^{13}C/^{12}C)_{reference}}\right) \times 1000‰\ VPDB \qquad 1\text{-}3$$

It is necessary to report the standard, or reference, used alongside the reported isotope values. Depending on the isotope system, difference standards are used. Bodies like the United Nations International Atomic Energy Agency (IAEA) and the National

Institute of Standards (NIST) collaborate to instigate, calibrate, and distribute the standards worldwide.

The physics behind stable isotopes is grounded in two principles: they do not undergo radioactive decay, but they do undergo fractionation (Urey, 1947; Bigeleisen and Mayer, 1947). Fractionation is the process whereby one isotope of an element is preferentially used in a process over another isotope based on the mass of the isotope. Because fractionation is a mass dependent process, the relative difference in mass between the isotopes must be large enough to be detected. There are fractionation effects in equilibrium, nonequilibrium (kinetic), and diffusive reactions (Clark and Fritz, 1995).

When a reaction achieves chemical equilibrium, by definition the forward and reverse reactions are proceeding at equal rates. Because of differences in dissociation energies between the heavy and light isotopes, the heavier isotope will react slower which leads to an enrichment of the heavier isotope in the less energetic phase. In karst processes, dissolved inorganic carbon, which contains isotopes of ^{13}C and ^{12}C, precipitates to form the mineral calcite. The mineral, constituting the solid and less energetic phase, therefore contains a greater concentration of the heavier isotope, ^{13}C (Drever, 1982; Clark and Fritz, 1995).

In kinetic fractionation, the masses of the isotopes involved in a reaction directly influence the kinetics of the reaction. When a system is moved from equilibrium, either the forward or reverse reaction rate will increase while the other will decrease. Depending on the reaction pathways, the fractionation is weakened or strengthened. If a reaction involves multiple products or reactants, either the light or the heavy isotope is preferentially involved in the reaction (Clark and Fritz, 1995).

When isotopes diffuse across a concentration gradient, fractionation occurs as a result of mass dependent velocities. The diffusion can occur in a different medium, such as the atmosphere or a plant leaf. The steady-state fractionation of two isotopes is dependent on their individual velocities which are calculated as follows (Clark and Fritz, 1995) where v refers to the molecular velocity (cm/sec), K is the Boltzmann constant (n $\cdot$ 1.380658 $\cdot$ 10^{-23} JK^{-1}, m is the molecular mass and T is the temperature (K).

$$v = \sqrt{\frac{KT}{2\pi m}} \qquad 1\text{-}4$$

To calculate the fractionation effect (α), Graham's Law is used to relate the velocities to thee respective masses. The heavier isotope is referred to as m* while the lighter isotope is m.

$$\propto_{m*-m} = \frac{\sqrt{\frac{kT}{2\pi m*}}}{\sqrt{\frac{kT}{2\pi m}}} = \sqrt{\frac{m}{m*}} \qquad 1\text{-}5$$

Because diffusive fractionation is unable to achieve equilibrium, it is characterized as a type of kinetic fractionation. If equilibrium were reached, there would be no fractionation.

Temperature Dependence

Temperature control on isotope fractionation is important to systems containing appreciable thermal fluctuations. For instance, when studying atmospheric and hydrologic effects in a climate that experiences a wide range of temperatures,

(Kentucky's yearly temperatures extremes can range from -17 to 32˚C) the temperature imparts a strong control on fractionation. Mathematically, the dissociation energy ratios are closer to one when the temperature is higher. Conversely, the energy term deviates from one when the temperature is lower. When the fractionation factor is close to one, there is little to no fractionation between isotopes. The important component occurs when temperatures decrease, because the fractionation factor diverges away from one and fractionation occurs. Applied to the carbonate system, Zhang et al. (1995) investigated the influences of temperature on the various carbonate species found in fresh waters (Fig. 1-6). As temperature decreases toward the left, the fractionation differences increase between the carbonate species.

Because stable isotopes are influenced by fractionation during physiochemical and diffusion processes, they are suitable for tracing various constituents and their sources. By measuring the sources, or inputs, to a system and comparing the inputs to the net output of a system, one may determine the sources of a chemical species in the system and determine the relative quantities of those sources. Isotopes behave in a mixing environment based on their mass and relative abundances, therefore allowing heterogeneous systems of particular isotopologues of certain elements to be used in identifying source contributions.

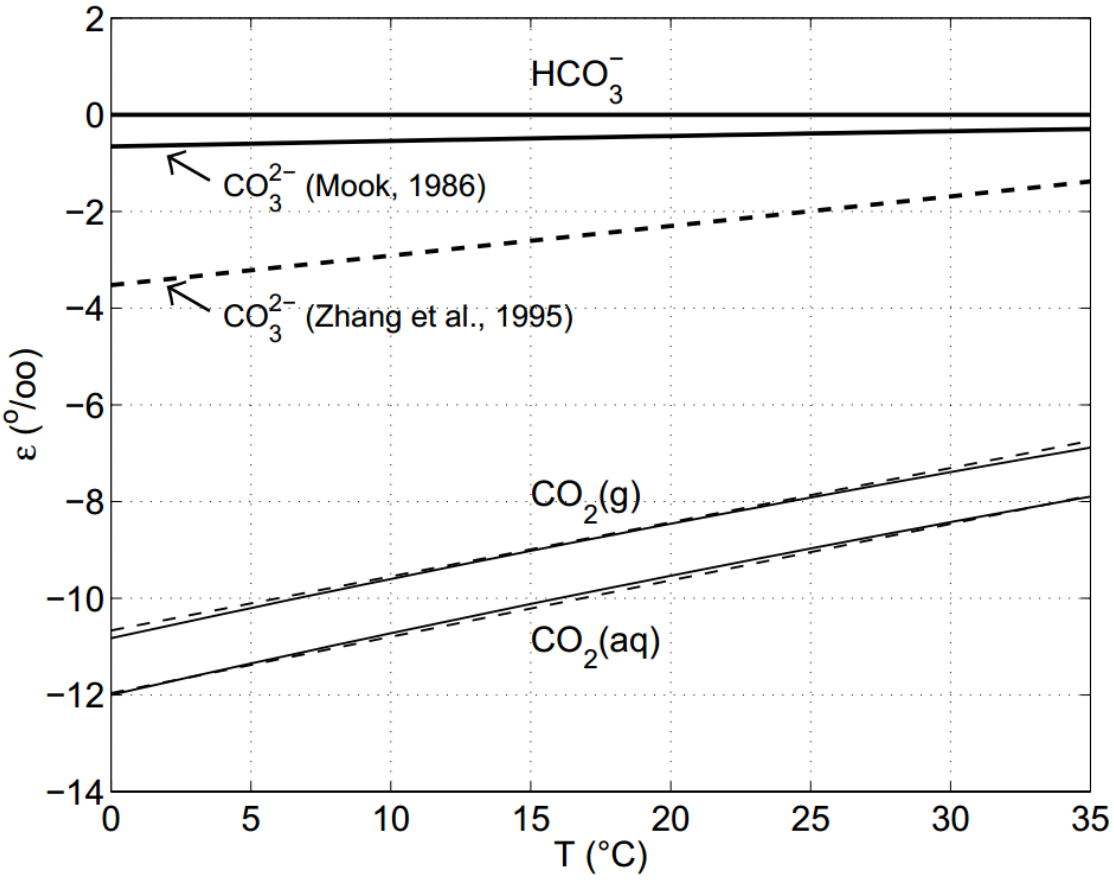

Fig. 1-6: Temperature influence on fractionation between carbonate species. As the temperature decreases, the fractionation differences increase.
Source: Adapted from Zeebe and Wolf-Gladrow (2001).

1.5 Riverine Carbon Cycle

Historically, carbon cycling and river geochemistry were studied through flux investigations (e.g., Degens et al., 1984). Recent advances in technology, however, allow these flux measurements to be combined with stable isotopes to examine the internal and external contributions of chemical species in addition to the concentrations (Pawellek et al., 2002; Barth et al., 2003; Das et al., 2005; Brunet et al., 2009; Tobias and Böhlke, 2011). Relative to river water, DIC is influenced by both internal cycles and

external inputs (Fig. 1-7) including vegetative effects, water-air exchanges of gases, hydrologic inputs, and the weathering of carbonate minerals (Redfield, 1958; Kling et al., 1992; Cox et al., 2000; Friedlingstein et al., 2001; Hope et al., 2001; Doctor et al., 2008).

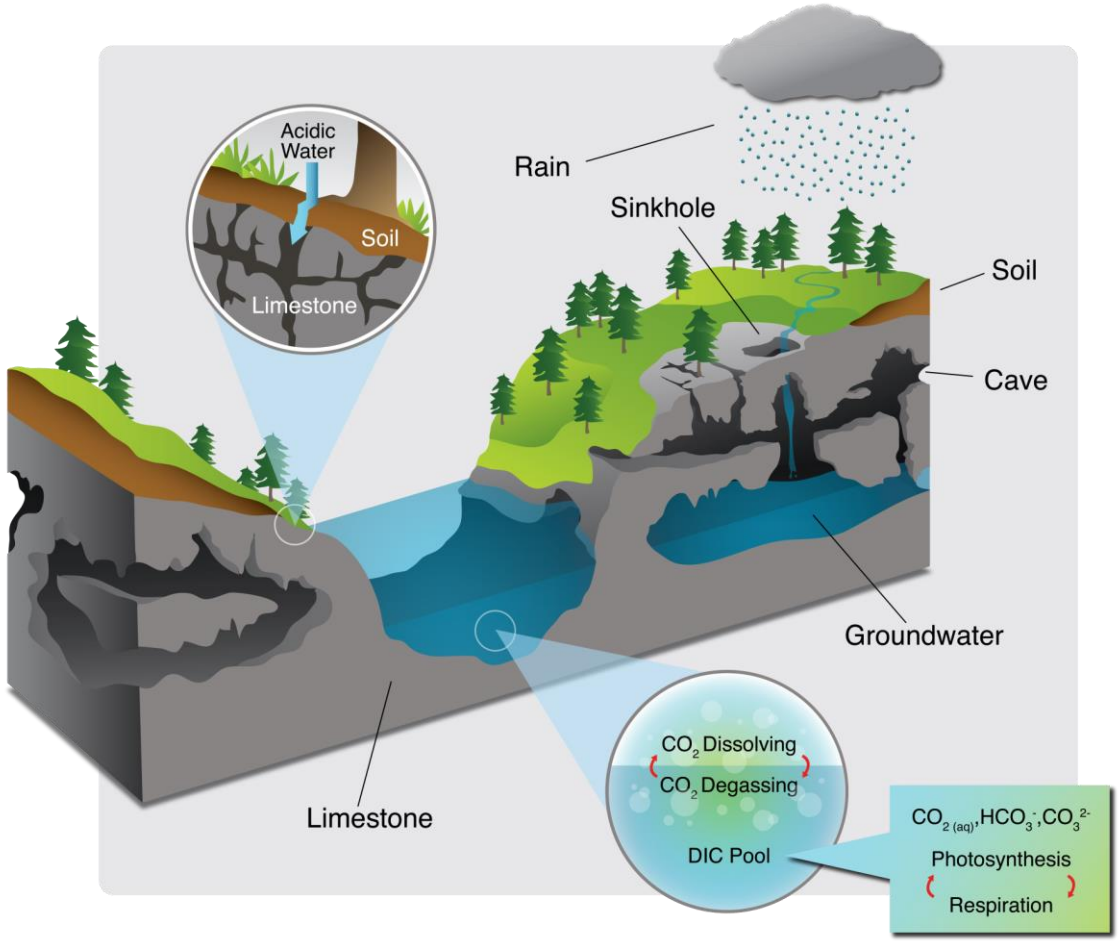

Fig. 1-7: Riverine carbon cycle of a karst influenced river. As acidic rainwater dissolves carbonate bedrock it transports inorganic carbon to the river. Inside the river, dissolving/degassing of CO_2 and photosynthesis/respiration cycles influence carbon cycling and fluxes. Source: Created by Jonathan Oglesby at WKU.

The upper Green river's aquatic and riparian vegetation can heavily influence the input and extraction of DIC through photosynthesis/respiration cycles. The Green River Dam also imparts a strong control on the hydrologic system and the partial pressures of

dissolved carbon in the river. The upstream hydrology is less influenced by karst development; however the Green River Dam modifies the river's natural flow and storm response. Downstream, the more developed karst aquifer under the Pennyroyal Plateau allows groundwater less restricted travel and direct contact with carbonate bedrock. This direct contact with limestones and dolostones allows groundwater to bring high fluxes of DIC to the river.

Vegetative Effects

Rivers with healthy aquatic life and biodiversity often show seasonal and diel CO_2 cycles (Parker et al., 2010), which are mainly influenced by primary producers and microbial activity. The main forcing is the fluctuation between photosynthesis and respiration in the vegetation and microbes (Pogue and Anderson, 1994; Parker et al., 2007). Vegetation in rivers consumes CO_2 and produces CO_2 through photosynthesis and respiration, respectively. Seasonality is shown to be important to this cycle as it can produce a 1‰ increase in $\delta^{13}C_{DIC}$ values during the warm season when productivity is higher (Pawellek and Veizer, 1994; Yang et al., 1996). Concurrent with seasonal controls, diel cycles of $\delta^{13}C_{DIC}$ exist because of the photosynthetic dependence on solar radiation. Tobias and Böhlke (2011) found that the $\delta^{13}C_{DIC}$ diel signature in a carbonate-dominated stream varied from -8 to -5‰, which is characteristic of other streams that are controlled by in-stream photosynthesis/respiration (Finlay, 2003; Parker et al., 2010). However, it is still not well known how these values vary under different geologic, hydrologic, and climatic conditions in most regions, particularly well-developed karst regions such as south-central Kentucky.

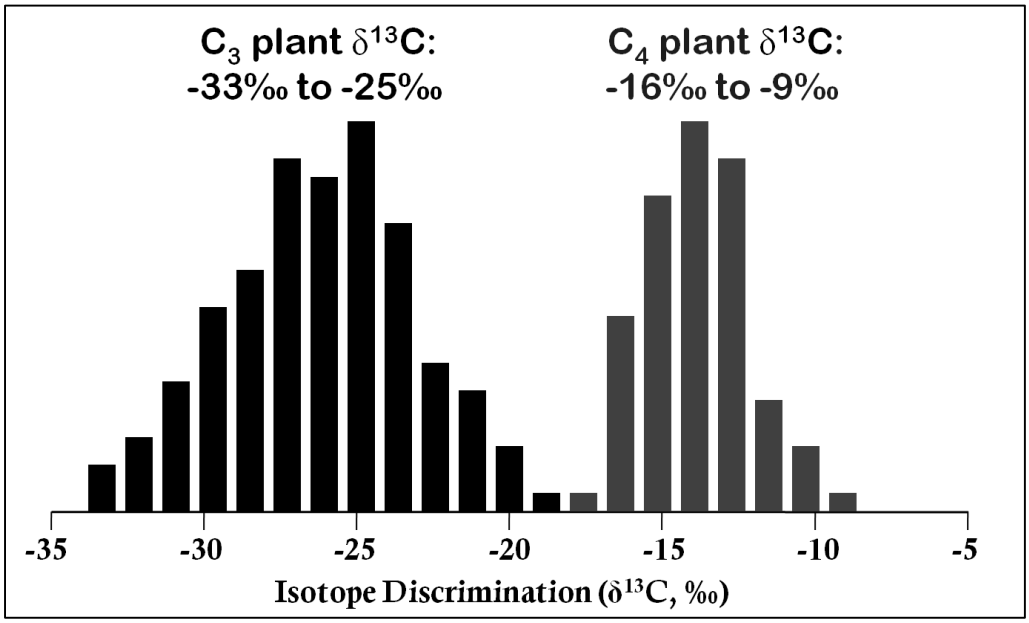

Figure 1-8: Differences in ^{13}C uptake between C_3 and C_4 plants.
Source: After Schwartz et al. (1986).

Photosynthesis by autotrophs involves the uptake of CO_2 and an accompanied depletion of ^{13}C. This depletion is due to diffusion of carbon into the plant, dissolution into the cell sap, and carbon fixation. As a result of these processes, ^{13}C is depleted by 5 to 25‰. The fractionation depends on the specific photosynthetic pathway (Fig. 1-8). There are three types of pathways: the Calvin (C_3) cycle (-24 to -30‰), the Hatch-Slack (C_4) cycle (-10 to -16‰), or the Crassulacean acid metabolism (CAM) cycle (-10 to -30‰) (Cerling et al., 1991; Fritz and Clark, 1995).

The three different types of vegetation prefer certain climatic regimes. C_3 plants dominate temperate, subtropical, and tropical regions (e.g., Kentucky is a subtropical region), C_4 plants dominate temperate grasslands, and CAM plants dominate deserts. Additionally, C_3 plants include crops such as wheat, rye, barley, and tobacco, while corn and sugar cane utilize the C_4 pathway (Clark and Fritz, 1995). Because CAM plants do

not exist in the region of south-central Kentucky, they were not investigated during this study. While the individual photosynthetic pathways are well studied, the contributions from each pathways into the Green River are not well constrained.

Water-Air Gas Exchange

Natural waters, including rivers, contain high concentrations of dissolved CO_2, which interacts with the overlying atmosphere. Dissolved CO_2 in natural waters is measured in partial pressures (pCO_2) and rivers typically contain higher partial pressures of CO_2 than the atmosphere. This increase in pCO_2 typically results in degassing of CO_2 along the stretch of the river unless the river originates from or flows through a large standing body of water (e.g. lake, reservoir). When the water column has a prolonged residence time in a lake, CO_2 degassing can allow the pCO_2 to reach equilibrium with the overlying atmosphere (Yang et al., 1996; Barth and Veizer, 1999; Aucour et al., 1999). It is possible for the pCO_2 to increase downstream as new ground and surface water inputs introduce water with higher pCO_2 levels to the river (Flintop et al., 1996). Alternatively, if the river transitions from silicate lithologies to carbonate lithologies, pCO_2 is able to increase due to carbonate precipitation/dissolution (Schulte et al. 2011). This is an important consideration with the impoundment of the Green River Lake Dam upstream of the portion of the river in this study. It is not well known how the transition from primarily siliciclastic bedrock to carbonate bedrock will affect the pCO_2 levels in the Green River, and subsequently the carbon isotope ratios due to varying input sources.

Hydrologic Inputs

As the Green River flows west through south-central Kentucky, it encounters the highly karstified Pennyroyal Plateau with numerous karst groundwater inputs into the system. In a river, $\delta^{13}C_{DIC}$ (mainly HCO_3^-) is controlled primarily by the influx of groundwater and matches isotopic ratios consistent with the weathering of carbonate minerals (Parker et al., 2010; Tobias and Böhlke, 2011). Before interacting with the calcite matrix, groundwater will adopt the $^{13}C/^{12}C$ ratio of the soil CO_2 during the acidification of precipitation. When groundwater interacts with the carbonate matrix, ^{13}C is enriched due to the relatively enriched state of carbonate minerals (0-2‰ VPDB) (Gonfiantini and Zuppi, 2003). Conversely, Parker et al. (2010) found that groundwater contributions of DIC were minimal in regards to controlling diel variations in $\delta^{13}C_{DIC}$. The direction and magnitude of influence of groundwater flux on $\delta^{13}C_{DIC}$ in karst riverine systems is still undetermined.

Carbonate Reactions

Carbonate reactions are crucial to quantifying DIC cycling in surface waters, especially in systems with high alkalinity (Spiro and Pentecost, 1991) and high primary productivity; karst landscapes are premier examples of this (Randerson et al., 1997; Aucour et al., 1999). Carbonate mineral precipitation and dissolution can impact element and compound aqueous concentrations (Parker et al., 2010), and the net effect of carbonate precipitation and dissolution can influence the flux of inorganic carbon delivered to oceans (Raymond and Cole, 2003; Szramek and Walter, 2004).

Together, the five controls on DIC, especially air-water interactions, in riverine systems influence the DIC budget over diel to seasonal timespans based on the primary productivity, extra-basinal organic carbon levels, and the nature of the local geology (Waldron et al., 2009). Quantification of the DIC influences, such as variable concentrations and speciation in DIC, saturation with respect to carbonate minerals, carbon isotope ratios, and other major inorganic chemical species, is required to examine the individual inputs. Additional information is found through the use of chemical models and isotopic mixing models (Bade and Cole, 2006). It is important to note differences in internal system cycling of DIC over differing temporal scales and to separate internal and external system influences (Spiro and Pentecost, 1991). There is still a need to study rivers in diverse environments over differing temporal scales to improve the quantification of carbon fluxes through watersheds under various climatic and biogeochemical conditions (Tobias and Böhlke, 2011).

CHAPTER TWO: CARBON CYCLING DYNAMICS IN A MID-LATITUDE KARST INFLUENCED RIVER

2.1 Introduction

Quantification of the carbon cycle is necessary given the important role atmospheric carbon dioxide plays in controlling the Earth's climate. Of the various components in the carbon cycle, rivers are of utmost importance as they are the primary conduits for dissolved inorganic carbon (DIC) from terrestrial basins to the oceans (Meybeck, 1987; Amiotte-Suchet and Probst, 1993a; 1993b; 1995; Ludwig et al., 1996a; 1996b; Amiotte-Suchet et al., 2003; Brunet et al., 2009; Doctor et al., 2008). DIC represents the most significant carbon fraction in the river compared to the organic and particulate fractions (Brunet et al., 2009). Ludwig et al. (1996a; 1996b) estimated that rivers transfer one gigaton of inorganic carbon per year to ocean basins.

DIC is controlled by vegetative influences, water-air exchanges of gases, hydrologic inputs, and the weathering of carbonate minerals (Redfield, 1958; Kling et al., 1992; Cox et al., 2000; Friedlingstein et al., 2001; Hope et al., 2001; Doctor et al., 2008; Brunet et al., 2009). Each source can be distinguished isotopically based on differing $\delta^{13}C$ values. The two common photosynthetic pathways, the Calvin Cycle (C_3) and the Hatch and Slack Cycle (C_4), deplete the carbon to -27‰ and -13‰, respectively (Clark and Fritz, 1995). As water with dissolved CO_2 enters the river, the relative differences in pCO_2 of the river and overlying atmosphere typically cause CO_2 to degas from or dissolve into the river. The act of degassing or dissolving CO_2 fractionates the carbon. Groundwater brings DIC to the river mostly in the form of dissolved bicarbonate, carbonate, and carbonic acid ($CO_{2(aq)}$). This is especially true in a carbonate

karst terrain as the rapid dissolution kinetics of the carbonate bedrock allows more dissolved bicarbonate to be input to the river (Drever, 1982). Depending on the original source of the carbonate bedrock, the $\delta^{13}C_{DIC}$ signature will vary. Marine carbonates are typically 0‰ while freshwater carbonates can range from 30‰ to 15‰ (Clark and Fritz, 1995). The $\delta^{13}C_{DIC}$ signatures of the various inputs will establish the sourcing of carbon, transport through a river, and the eventual fate of DIC in a river.

The regionally important Green River in south-central Kentucky represents the most biodiverse area in the Ohio River system and is the hydrologic base level for the region (USACE, 2011). Within this region lies the world's current longest known cave, the Mammoth Cave System. The Green River flows east to west from the spine of the Cincinnati Arch toward the Illinois Basin, where it becomes a tributary of the Ohio River. The headwaters gather over siliciclastic dominated stratigraphy with limited karstification. To the west, the river cuts into a carbonate plateau with a highly developed karstified aquifer. Karst landscapes like south-central Kentucky play important and relatively unstudied roles in atmospheric carbon uptake (Esser et al., 2010; Davidson et al., 2010). Nevertheless, few, if any, measurements exist for carbon cycling within this river system, which may play an important role in nutrient transport. This study focused on the $\delta^{13}C_{DIC}$ character of the river over seasonal timespans to establish baselines for carbon sourcing, transport and fate along the river through the following questions:

- How do interannual and seasonal changes in riparian vegetation and basin hydrology impact the inorganic carbon sourcing along the upper Green River?

- How does carbon sourcing vary between a more siliciclastic, less karstified catchment and a more carbonate rich, heavily karstified catchment?

2.2 Study Area

The upper Green River represents the hydrologic base level for the region. Four tributaries (the Barren, Nolin, Pond, and Rough) and over eighty springs flow into the Green River (Benke and Cushing, 2005). The upper Green River flows east to west (Fig. 2-1) from more siliciclastic bedrock (Fort Payne Formation) to a heavily karstified limestone plateau, known locally as the Pennyroyal Plateau (St. Louis and St. Genevieve Formations). This geologic framework is critical to furthering our understanding of riverine carbon dynamics. While many geologic studies are set up on monolithic basins, the majority of rivers transect multiple lithologies. The differences in site characteristics provided the foundation for gathering insight to carbon cycling over varying terrains in terms of both hydrology and mineral weathering processes (Fig 1-2).

The Green River represents the most biologically diverse river within the Ohio River system. The study section for this research, located between Greensburg and Munfordville, contains the greatest species diversity within the river. The U.S. Fish and Wildlife Service lists seven species within the Green River system as endangered, in addition to several ecosystems (KGRCREP, 2010).

The upstream nested basin drains 1,919 km^2 over heterogeneous lithologies. Devonian shales and Mississippian limestones comprise the majority of the upstream basin's surficial geology. Select areas of the basin contain Ordovician dolostones, Mississippian sandstones, and Pleistocene and Holocene sands (Osterhoudt, 2014). The

downstream basin includes the nested upstream basin increasing the total drainage area to 4,489 km^2 (Osterhoudt, 2014). The downstream basin contains more homogeneous surficial lithologies. Surficially, the majority of the basin is composed of the same Mississippian carbonates that form the Mammoth Cave System (Fig. 1-3) (Palmer and Palmer, 2009). The lower basin also includes small outcrops of shales, sandstones, and siltstones (Osterhoudt, 2014). South-central Kentucky receives an average of 122 cm of precipitation per year with an average atmospheric temperature of 13.83°C (KCC, 2013). Kentucky experiences pronounced wet/dry seasonality with 60% of precipitation occurring in the summer and 40% in the winter (Hess and White, 1988). In response to this annual precipitation pattern, the upper Green River's discharge averages 37,479 L/s in Greensburg and 82,098 L/s in Munfordville (USGS, 2013).

2.3 Methods

Two sites were established along a 110-kilometer stretch of the Green River in the towns of Greensburg and Munfordville, KY (Fig. 2-1 and 2-2). The difference in karstification between the upstream and downstream locations allowed a comparison to be developed between the two sites, in addition to gaining insight into the influence of differing lithologies on the carbon cycling within the river. The Green River Dam created a unique situation by potentially altering the river chemistry through increased residence time, stagnation, and allowing the dissolved CO_2 to degas from the river and affect pH and dissolved carbonate speciation.

Fig. 2-1: Looking north across the Green River at Greensburg.
Source: Photo by author.

Fig. 2-2: Looking southwest at Green River at Munfordville.
Source: Photo by author.

Each river site included two Soilmoisture Equipment 1900L36-B02M2 soil water samplers (lysimeters) to characterize the soil respiration inputs to the river. Each lysimeter was located at a 90cm depth, with Lysimeter 1 located on the first flood bank and Lysimeter 2 located on the second flood bank. Two lysimeters provided redundancy to the data collection in case of flooding events, malfunctions, or human intervention.

To collect groundwater from each catchment, two groundwater wells were utilized. The Greensburg well is located 10 km south of Greensburg on private property; the Munfordville well is located on the Western Kentucky University Green River Preserve.

River water samples were collected from the center of the river, conditions permitting. A pedestrian-friendly bridge in Greensburg was regularly accessed to collect samples. A similar bridge near the Munfordville site was not pedestrian accessible so only during base flow were samples able to be collected from the center of the river. When conditions necessitated collecting samples from the river's edge, samples were collected so as to maximize the distance from riparian vegetation in an effort to reduce direct soil water influences.

Carbon isotope samples collected between June 23rd, 2013, and January 7th, 2014, were collected in 5.9 ml exetainers with septa caps. The remaining samples (January 14th through May 12th, 2014) were collected in 10 ml sample vials with no septa caps. All samples were capped with no airspace, parafilmed, and refrigerated to 4°C with no preservatives (Doctor et al., 2008). The carbon isotope samples switched containers due to a forced change in analysis laboratory. Concurrent to sample

collection, a YSI 556 multiparameter sonde was used to record the pH, conductivity, and temperature of the sample water.

Carbon isotope samples were analyzed at two different laboratories. All samples collected between June and October, 2013, were analyzed at the University of Kentucky Earth and Environmental Science's (UK-EES) Stable Isotope Geochemistry Laboratory. The remainder of the samples was analyzed under the same conditions at the University of Utah's Stable Isotope Ratio Facility for Environmental Research (SIRFER). Analyses at both labs were performed by the same personnel using a Thermo Finnegan Delta Plus Isotope Ratio Mass Spectrometer model with a gas bench. The results were reported in standard δ notation with a precision of ±0.1‰. Results are referenced to the Vienna Pee Dee Belemnite (VPDB) standard.

Using a combination of observational data collected from the grab samples with established values for atmospheric and carbonate bedrock $\delta^{13}C_{DIC}$ values, a mixing model was run to predict specific source contributions over various timescales. For this study, the program IsoSource (v1.3) produced by Don Phillips of the United States Environmental Protection Agency was used (Phillips and Jillian, 2003).

The model was run for each week's data for which all sources were analyzed. This caused a gap in the Munfordville site's mixing model because the groundwater samples were unobtainable throughout the majority of the spring season. For those weeks with complete data sets, the model was run with a 1.0% increment and a mass balance tolerance of 0.5‰. The model is mathematically underdetermined as it includes only one isotope system with four sources. The four sources included: (1) groundwater, (2) soil respiration, (3) atmosphere, and (4) carbonate reactions. The groundwater and

soil respiration data were input from the analysis of samples collected during this study, while the atmosphere and carbonate reaction inputs were assumed constant and based on the established literature. For all weeks, the atmosphere was assumed to be -9.0‰ (Zhang et al., 1995) and carbonate reactions (bedrock sources) were assumed to be 0.0‰ (Clark and Fritz, 1995).

The model outputs presented the feasible ranges of isotope contributions given mass balance with qualitative statistics (mean, minimum, maximum, standard deviation). To avoid misinterpreting the model results, the standard deviations and ranges of possible solutions were utilized. Median values were calculated for each week's mean solution. Additionally, when calculating seasonal changes, median values were calculated for each source and reported with standard deviations. All statistical treatments were performed in Systat Software's SigmaPlot v11.0 and Microsoft Office Excel 2010.

2.4 Results

A total of 237 samples were collected for $\delta^{13}C_{DIC}$ analysis during the period from June, 2013, to May, 2014. These data span the seasonal influence on the Green and capture changes related to storm events, dam releases, and fluctuations in groundwater flow between the upstream and downstream reaches. Analyses were conducted on two timescales: (1) the entire year from June, 2013, to May, 2014, and (2) seasonal trends for fall 2013, winter 2013, and spring 2014. For these analyses, fall is considered between September through October, winter is November through February, and spring is March through May. Summer 2013 (June through August) was not analyzed in this study

because the river input sampling needed for the mixing model was not available until the fall of that year.

Time Series Analysis of $\delta^{13}C_{DIC}$ and pH

A time series of the isotopic data is presented in Figures 2-3 and 2-4. Dissolved inorganic carbon isotopes showed a distinct seasonal trend between summer and winter. The upstream site showed more depleted values, averaging –14.88‰, with a range of –15.2‰ to –6.5‰ in the late summer (June, July, August). In the winter months (November, December, January), the $\delta^{13}C_{DIC}$ was enriched by ~2.7‰ on average yielding an average of –12.1‰, with a range of –10.7‰ to –14.1‰. Downstream, at Munfordville, the river showed a similar trend. The summer $\delta^{13}C_{DIC}$ data had an average of –14.4‰ with a range of –17.7‰ to –12.6‰. In the winter, the range enriched to –13.7‰ to -4.1‰ with an average of –11.2‰. The pH of the river at both sites showed little seasonal change possibly due to sampling occurring at various hydrologic conditions throughout the year.

River Geochemistry and Hydrology

The upstream site showed pH values ranging from 5.5 to 6.7, with an average of 6.77 (Fig. 2-5 A). The downstream site ranged from 5.54 to 8.17, and averaged 7.01 (Fig. 2-5 B). The specific conductivity of the river at Greensburg ranged from 98 µs/cm (March) to 303 µs/cm (July) with an average of 167 µs/cm (Fig. 2-5 C). Munfordville had a minimum specific conductivity of 144 µs/cm (October) and a maximum of 374 µs/cm (December) with an average of 241 µs/cm (Fig 2-5 D). These trends of slightly

higher pH and specific conductivity were consistent with the buffering capabilities and dissolution kinetics of more carbonate dominated lithology downstream. The water temperatures at Greensburg reached a minimum of 0.33° C in winter and a maximum of 27.6° C in summer and averaged 14.6° C (Fig. 2-5 E). Munfordville's water temperatures ranged from 0.45° C to 28.5° C *from winter to summer*, respectively. The average water temperature was 15° C (Fig. 2-5 F) (Osterhoudt, 2014).

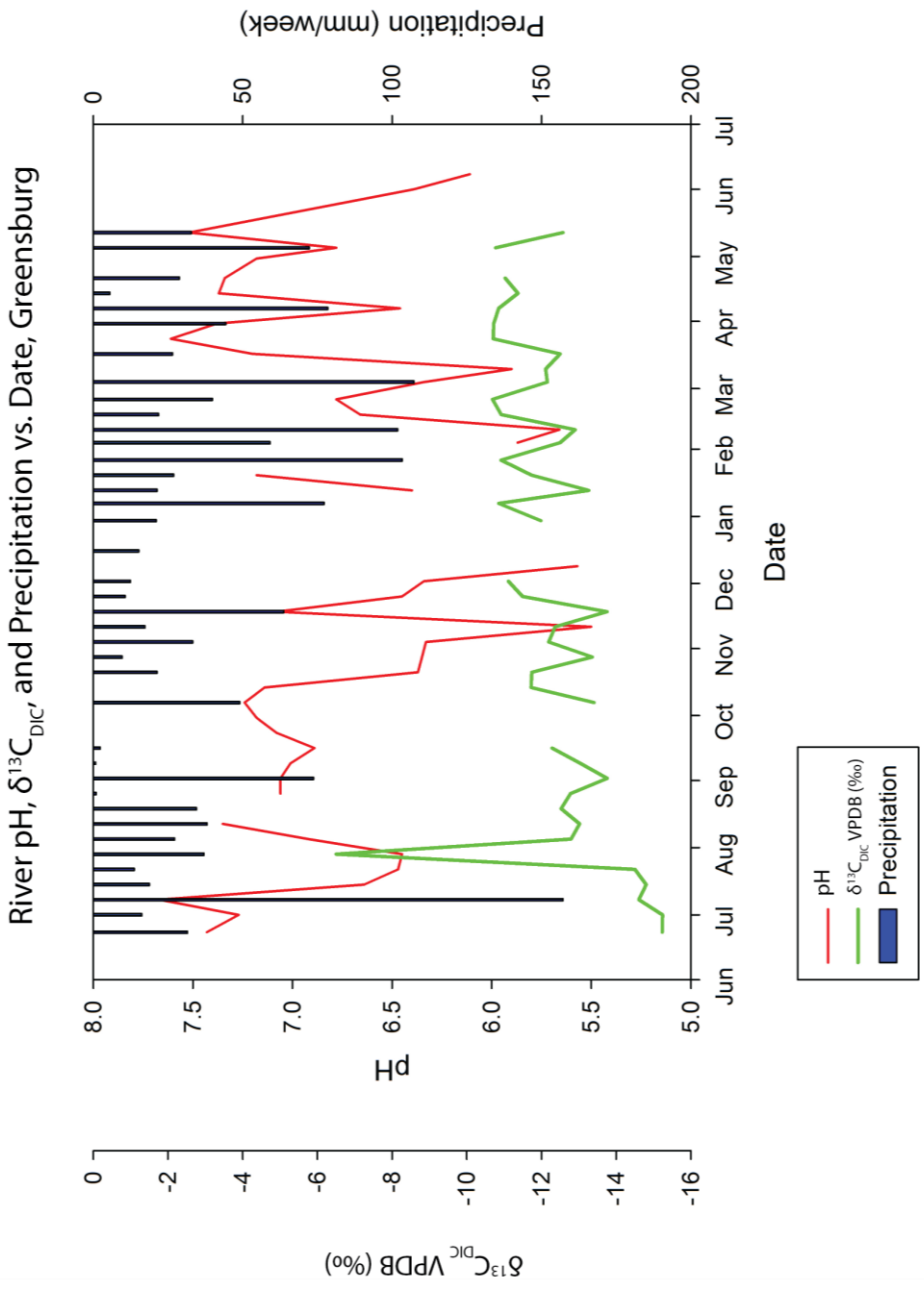

Fig. 2-3: Time series of river pH and $\delta^{13}C$ at Greensburg with basin precipitation for reference. Source: Created by the author.

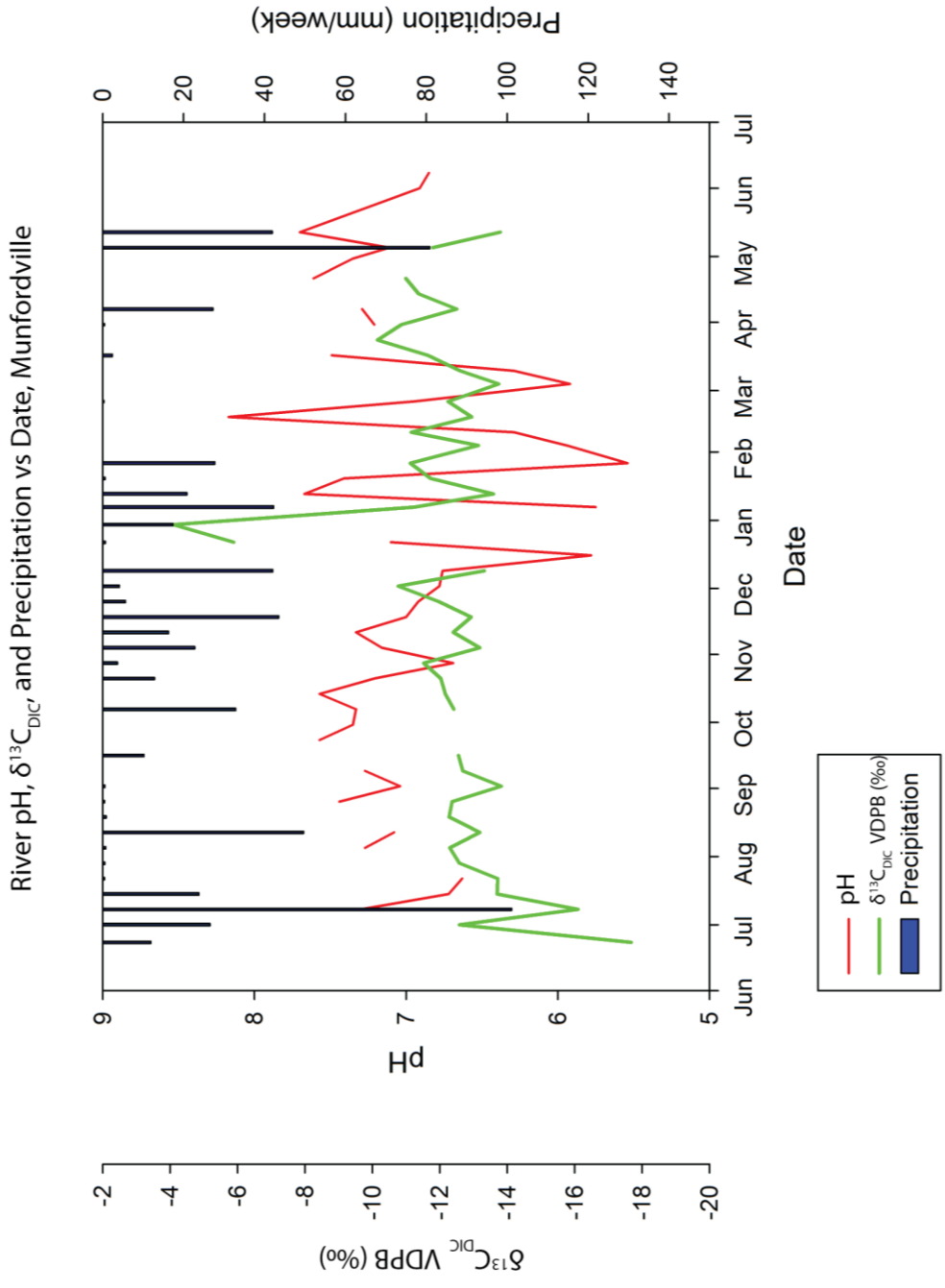

Fig. 2-4: Time series of pH and $\delta^{13}C$ at Munfordville with basin precipitation for reference. Source: Created by the author.

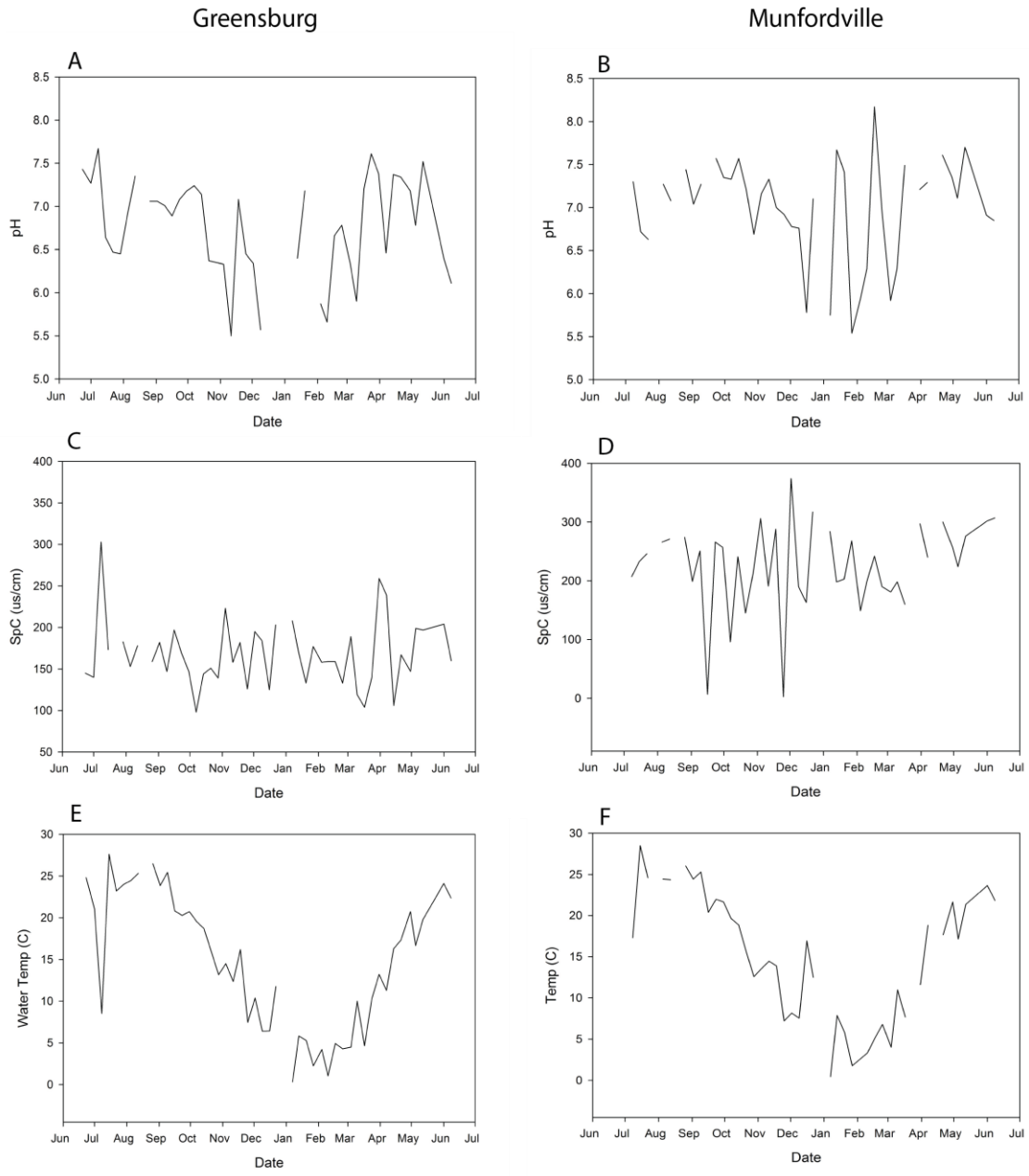

Fig. 2-5: Geochemistry (pH, SpC, and temperature) of both field sites. Note the general lack of seasonality, excluding the temperature data. Both sites exhibited similar ranges in pH, conductivity and temperature throughout the year.
Source: Created by the author.

The discharge at Greensburg and Munfordville (Fig. 2-6 A-B) displayed a seasonal trend paralleling that of $\delta^{13}C_{DIC}$ in the river, with lower discharges in the fall and early winter and pronounced increases heading into the spring. In the fall, the discharge averaged 30,700 L/s at Greensburg (Fig. 2-6 A) and 46,400 L/s at Munfordville (Fig. 2-6 B). The maximum and minimum discharges at each site were 192,800 L/s at Greensburg and 253,200 L/s at Munfordville. In the spring, the discharges averaged 92,900 L/s and 186,000 L/s at Greensburg and Munfordville, respectively. These trends were consistent with a larger drainage basin downstream in addition to more pronounced discharge from karst springs along the downstream reach.

Green River Dam

A potential control on riverine geochemical and isotopic cycles was the Green River Dam located upstream of Greensburg. Figure 2-7 shows the daily dam release fluxes (red hatched data) from July, 2013, through June, 2014, alongside the reservoir gauge height (black data) and local precipitation records (blue data). Due to data availability limitations for the dam releases, the raw data were unavailable for analysis, thus making descriptive statistics difficult at best. However, there was still a seasonal trend coinciding with the late summer/fall and spring. Increased precipitation upstream of the dam facilitated larger dam releases in the spring. The increased residence time of reservoir water may have altered the geochemistry and allows the DIC to equilibrate with atmospheric CO_2. This phenomenon may provide valuable insight to isotopic and geochemical outliers.

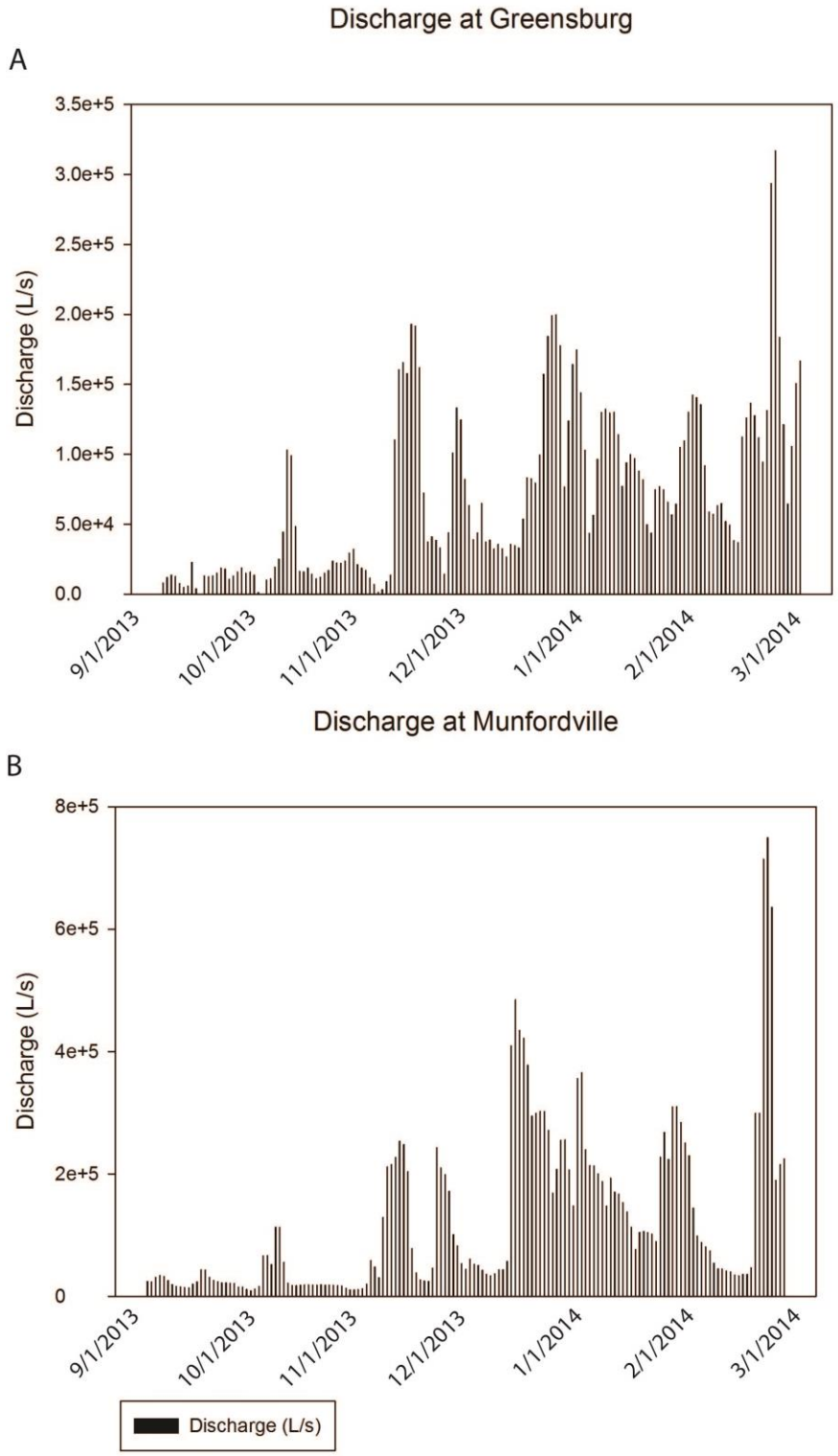

Fig. 2-6: Discharge fluxes at Greensburg (A) and Munfordville (B). Note the seasonality in discharge with lower values in the late fall/winter and higher discharges in the spring. Source: Created by the author.

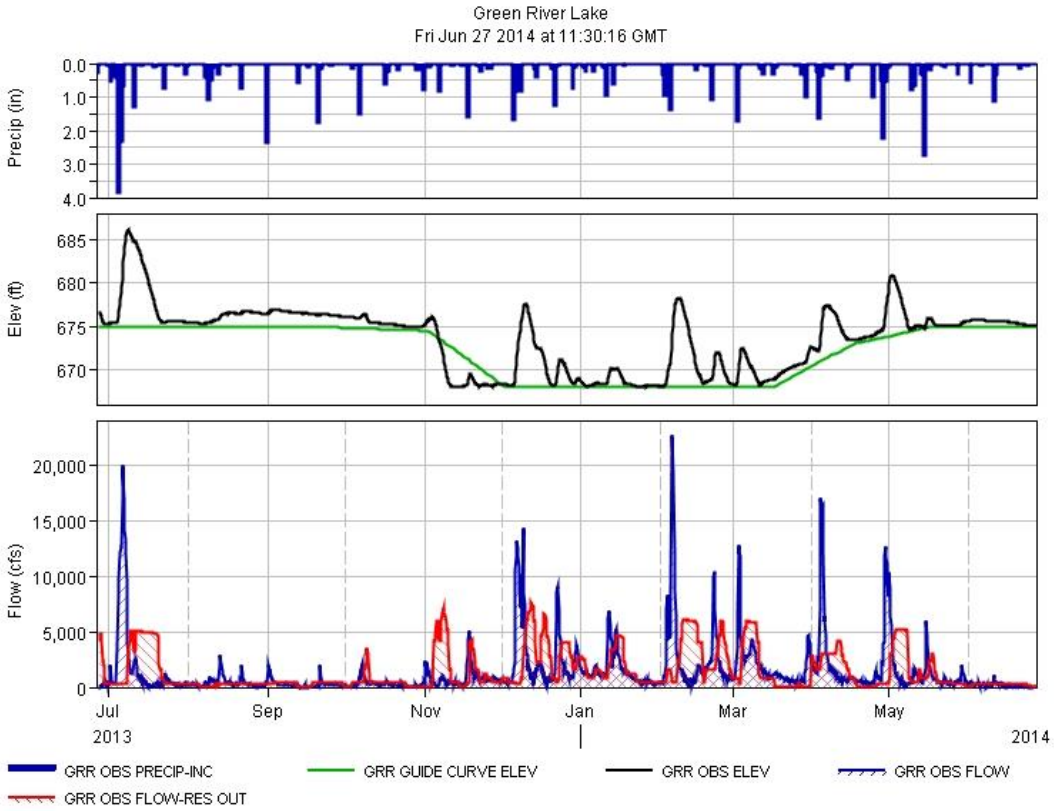

Fig. 2-7: Green River Lake discharge, stage height, and local precipitation records for the study period. Source: USACE (2011).

Mixing Model Results

The data for each sample collection date were entered into *IsoSource*, a mixing model program. Data for the river mixture, groundwater input, and soil water varied week to week. Due to having two lysimeters at each site, the soil water data were averaged when both lysimeters produced samples. Atmospheric and carbonate reactions were entered into the model as constants. The atmosphere is currently -8‰ VPDB and carbonate mineral reactions were assumed to be 0‰ (Dubois et al., 2010; Clark and Fritz, 1995). The model assumed there is no fractionation between the DIC sources and

the river mixture. This was not true with atmospheric CO_2 dissolving into the river. The kinetic fractionation effects during CO_2 dissolving into surface waters, depleted the signal by ~1.0‰ (Zhang et al., 1995) making the model input ~9.00‰ (VPDB).

Time series analysis showed a noticeable change in the model outcomes occurs in January, 2014, which coincided with the change in sampling method. No data existed for spring in Munfordville due to restricted access to the groundwater samples. In Greensburg, the model predicted over 90% of DIC originated from soil water during the middle of winter when photosynthetic activity is at a minimum. Similarly, in February, when the year's highest precipitation rates occurred, groundwater contributed 2.5% of all DIC. Similar trends were noticed in Munfordville. Using the raw results, the model predicted over 70% of total DIC originated from soil water during the middle of winter when photosynthetic activity is at a minimum. This change in sourcing occurs with no appreciable change in the local environmental factors. This time period also recorded the lowest water temperatures with values approaching 0°C indicating fractionation will be at a maximum.

Corrected Mixing Model Annual Trend

The corrected mixing model results (Appendix B) from *IsoSource* are displayed in Figures 2-9 and 2-10 for Greensburg and Munfordville, respectively. Isotope samples collected on or before January 7, 2014, were sampled in 5.9 ml exetainers. All samples after this date were collected with an alternative vial that, unknown at the time of collection, did not seal well against the atmosphere, allowing possible fractionation due to gas exchange. To compensate for this, correction values were applied to the post-

January 7, 2014, sample data. Each isotope source's data were corrected using the existing offset from the last correct data point before the vial switch occurred. This method best preserved the residual long-term trends and fits within accepted correction practices.

In Greensburg, the median contribution of groundwater to the river was 33.2 ± 22.6% with a minimum of 20.5% and a maximum of 34.9%. Soil contributed a median value of 33.6 ± 13.0% with a minimum and maximum of 20.9% and 63.4%. The median atmospheric contribution was 23.0 ± 16.7% with a range of 11.6% to 29.8%. The median in-situ carbonate reaction contribution was 11.2 ± 7.7% with a minimum observed of 4.5% and a maximum of 16.4% (Fig. 2-8) .

The median observed groundwater contribution to DIC in Munfordville was 22.6 ± 16.4% with a range of 15.5% to 25.5%. Soil contributed a minimum of 6.8% and a maximum of 47.2% with a median of 37.3 ± 7.2%. The atmosphere represented a median contribution of 23.2 ± 16.8% with a range of 15.2% to 26.8%. In-situ carbonate reactions provided a median contribution of 13.2 ± 9.6% DIC on average, with as little as 10.0% and a much as 62.5% contribution pending the season and influence of storm events (Fig. 2-9).

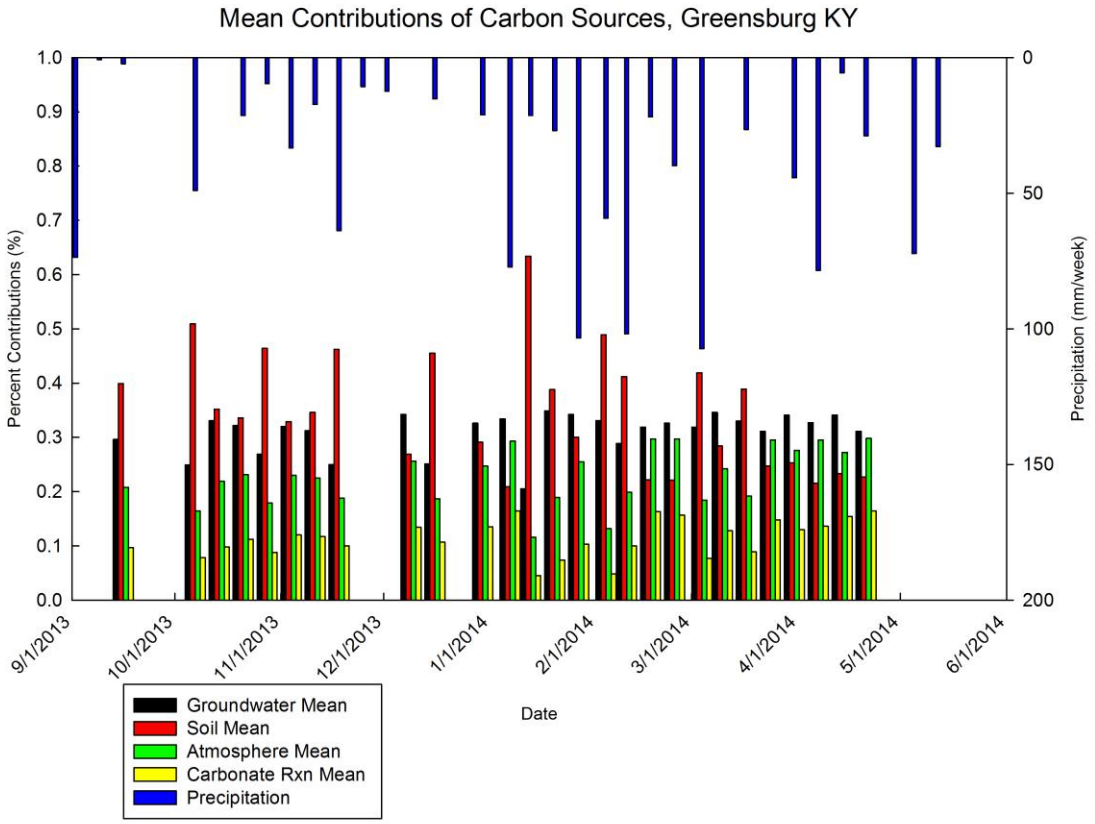

Fig. 2-8: Time series of mixing model results for Greensburg. Note the consistently high contributions of soil water and groundwater DIC to the river.
Source: Created by the author.

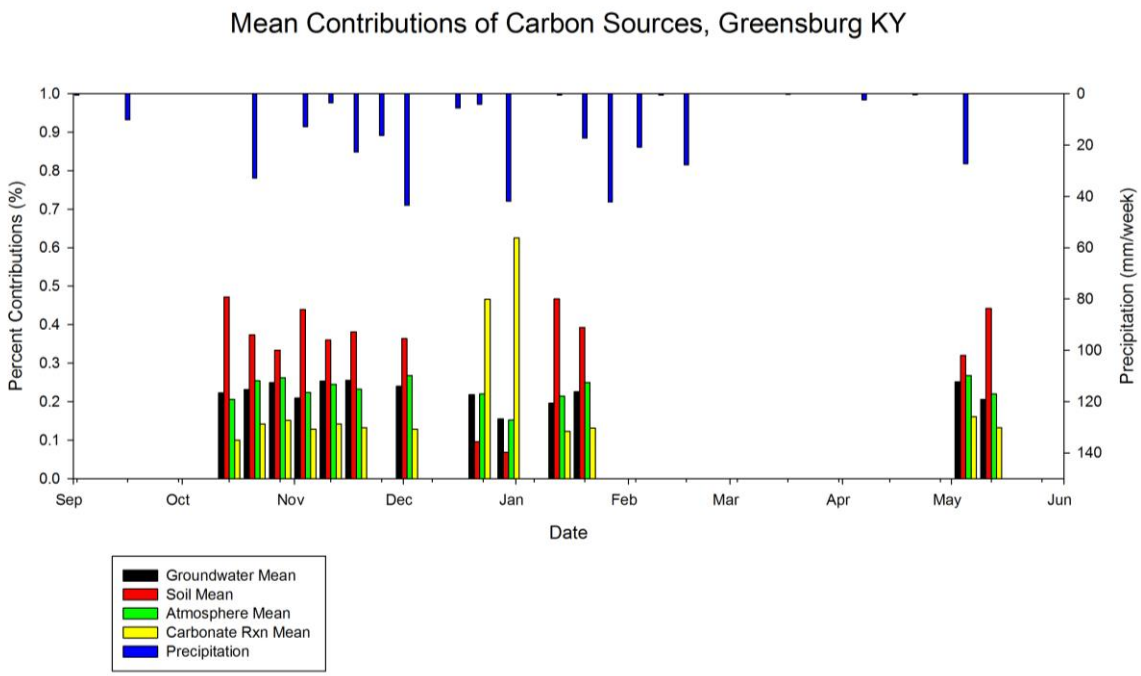

Fig. 2-9: Time series analysis of mixing model results for Munfordville. The gap of data in the spring is a result of limited access to groundwater samples.
Source: Created by the author.

Corrected Mixing Model Seasonal Trends

Seasonal trends are summarized in Tables 2-1 and 2-2. To represent the model results more accurately, the median values of the model averages are reported with standard deviations and the range of possible solutions. In the upstream basin, riparian soil water contributed the highest median concentrations of DIC in the fall (39.9 ± 12.9%), likely from throughflow of infiltrating water along the slopes. The smallest source of DIC was in-situ carbonate reactions within the river (9.7 ± 6.6%). In spring, the highest average source of DIC shifted to groundwater (32.9 ± 23.2%), while the in-situ carbonate reactions still contributed the least (13.3 ± 9.0%). In Munfordville, the largest DIC source in the fall was also soil water (37.3 ± 7.6%), while carbonate

reactions produced the lowest concentrations of DIC (14.2 ± 10.4%). Unfortunately, no data existed for the spring due to limited access to the groundwater sampling location. Here, the groundwater produced slightly less DIC than Greensburg. Soil water also showed a more stabilized pattern season to season with median contributions between 30-40%.

Table 2-1: Seasonal trends of corrected mixing model for Greensburg. Note the groundwater consistently produces one third of the DIC while the soil water is far more variable in its contributions.

		Greensburg DIC Contributions by Source							
		Groundwater		Soil		Atmosphere		Carbonate Reactions	
		Value	Median Std	Value	Median Std	Value	Median Std	Value	Median Std
Fall	Median	29.60%	19.30%	39.90%	12.90%	20.80%	15.00%	9.70%	6.60%
	Min	24.90%		33.60%		16.40%		7.80%	
	Max	33.10%		50.90%		23.10%		11.20%	
Winter	Median	32.30%	22.50%	33.75%	12.15%	22.75%	16.50%	11.20%	8.15%
	Min	20.50%		20.90%		11.60%		4.50%	
	Max	34.90%		63.40%		29.70%		16.40%	
Spring	Median	32.85%	23.20%	25.00%	14.00%	27.40%	19.15%	13.30%	9.00%
	Min	31.10%		21.50%		18.40%		7.70%	
	Max	34.60%		41.90%		29.80%		16.40%	

Source: Created by the author.

Table 2-2: Seasonal trends of corrected mixing model results for Munfordville.

		Munfordville DIC Contributions by Source							
		Groundwater		Soil		Atmosphere		Carbonate Reactions	
		Value	Median Std	Value	Median Std	Value	Median Std	Value	Median Std
Fall	Median	23.10%	16.70%	37.30%	7.60%	25.40%	18.20%	14.20%	10.40%
	Min	22.30%		33.40%		20.60%		10.00%	
	Max	24.90%		47.20%		26.20%		15.10%	
Winter	Median	22.20%	16.10%	37.25%	7.40%	22.80%	16.50%	13.15%	9.40%
	Min	15.50%		6.80%		15.20%		12.30%	
	Max	25.50%		46.70%		26.80%		62.50%	

Source: Created by the author.

2.5 Discussion

Inorganic River Chemistry

As noted by other studies, there existed strong relationships between pH, specific conductivity, temperature, and hydrologic inputs in surface waters (Dicken, 1935; Katz et al., 1997; O'Driscoll and DeWalle, 2006; Hatcher, 2013; Palmer, 2007; Lawhon, 2014; Osterhoudt, 2014). Along the same stretch of the upper Green River, Osterhoudt (2014) noted an overall increase in pH due to an increasing percentage of carbonate bedrock at the downstream reach of the river. Carbonates, like silicates, remove CO_2 from a system through weathering; however, the kinetics behind carbonate dissolution cause carbonates to dissolve much quicker than silicates. Lasaga et al. (1994) experimentally determined the weathering time for 1mm spheres of various minerals exposed to weather. Their results showed calcite dissolved in 0.1 years while quartz was extrapolated to require 34,000,000 years to dissolve. This obvious difference in kinetics allows for increased removal of CO_2 (Drever, 1982). CO_2 is interpreted as carbonic acid, H_2CO_3 in aqueous systems, so as CO_2 is removed from the system, the pH is buffered to higher values (Drever, 1982; Katz et al., 1997; Palmer, 2007; Hatcher, 2013).

Specific conductivity (SpC), as a measure of dissolved and particulate ions (particularly dissolved and particulate carbon), is likely related to the chemical resistance of the basin soils and bedrock. More chemically resistant silicate bedrock upstream restricts the ionic concentrations in the river. This provided one explanation why Greensburg averaged 167 μs/cm during the study period (Fig. 2-5 C), while the more carbonate-dominated Munfordville site averaged 241 μs/cm (Fig 2-5 D). The higher SpC values downstream indicated high ionic content in the river water, likely

from enhanced dissolution of carbonate minerals.

During high precipitation, it would be expected that higher concentrations of dissolved ions would be present as fresh meteoric water flushes through the system dissolving bedrock. However, the opposite is observed in the Green River; during high discharge events, the conductivity decreases considerably. This was likely due to dilution effects from the increased baseflow and throughflow (Osterhoudt, 2014). In this case, the dilution effects overprinted the increased ionic fluxes (Lawhon, 2014). During the spring when more precipitation fell (Fig. 2-5 C,D), the conductivity records showed a greater range as high discharge storm events push through the system.

The water temperature records for both Greensburg and Munfordville indicated seasonal trends aligned with meteorological trends. The summer months had water temperatures in the 20-25°C range, which corresponded with the high atmospheric temperatures. During the winter months, as atmospheric temperatures decreased, the water temperature decreased accordingly (Fig. 2-5 E, F). This is an important consideration when working with isotopes since fractionation is temperature dependent. As temperature decreases, fractionation between species increases (Fig. 1-6) (Clark and Fritz, 1995). The recorded river temperatures at or near 0° C in the early months of 2014 involved the highest degrees of fractionation as carbonate speciation changed due to daily and seasonal pH fluctuations (Zhang et al., 1995). This period of quiescence, characterized by minimal vegetative influences, and seasonally low precipitation, maintained the highest range in $\delta^{13}C_{DIC}$ values for both Greensburg and Munfordville (3.4‰ and 3.9‰, respectively) (Fig. 2-3, 2-4).

The geological and hydrological differences between the basins limited the temperature variability of groundwater. It was found that meteorological influences exerted greater control on river temperatures in Greensburg due to limited spring input and longer groundwater residence times. Both of these related directly to the limited karstification found in the upstream basin. With a high degree of karstification and several large spring inputs nearby, Munfordville was shown to be largely controlled by groundwater temperatures as the groundwater residence times would be shorter (O'Driscoll and DeWalle, 2006; Osterhoudt, 2014). The Green River Dam also exerted influence on the system's geochemistry as a whole and will be discussed separately.

Comparison to World Rivers

Table 2-3 summarizes the carbon isotopic values for the upper Green River, along with several well-studied river systems around the world. Throughout the entire study period, both the upstream and downstream sites averaged a $\delta^{13}C_{DIC}$ of 12.2‰ with maximums occurring at -6.5‰ and -4.09‰ and minimums at -15.24‰ and -17.68‰ for the respective upstream and downstream sites. These results were consistent with several mid-latitude streams (Hitchon and Krouse, 1972; Atekwana and Krishnamurthy, 1998; Tellmer and Veizer, 1999; Amiotte-Suchet et al., 1999).

Table 2-3: Comparison of this study's results with other studies conducted around the world.

River	$\delta^{13}C_{DIC}$			Reference
	Mean	Max	Min	
Kalamazoo (USA)	-10.42	-8.7	-13.7	Atekwana and Krishnamurthy, 1998
Owens Creek (USA)		-9	-15	Kendall et al., 1992
Shelter Run (USA)		-11	-20	Kendall et al., 1992
Fraser (Canada)	-6.04	-3.57	-10.2	Cameron et al., 1995
St. Lawrence (Canada)	-5.12	0.7	-16.5	Yang et al., 1996
	-4.66	0.3	-13.7	Barth et al., 1998
	-4	2.2	-13.3	Barth and Veizer, 1999
	-5.9	0.11	-14.21	Hèlle et al., 2002
Ottawa (Canada)	-10.43	7.3	-17.4	Telmer and Veizer, 1999
Mackenzie (Canada)	-11.82	5.7	-24.4	Hitchon and Krouse, 1972
Amazon (Brazil)		-11.8	-28.5	Longinelli and Edmond, 1983
Orinoco (Venezuela)		-11.3	-20.1	Tan and Edmond, 1993
Strengbach (France)	-16.68	-9.3	-24.4	Amiotte-Suchet et al., 1999
Rhoene (France)	-8.91	-2.2	-13	Aucour et al., 1999
Rhine (Germany)	-8.8	-4.4	-14.4	Buhl et al., 1991
	-10.14	-4	-17.1	Flintop et al., 1991
Danube (Austria)	-6.92	0.3	-11.4	Pawellek and Veizer, 1994
Ganges Brahmaputra (India)		3.9	-12.7	Galy and France-Lanord, 1999
Indus (Pakistan)	-3.21	0.6	-9.6	Karim and Veizer, 2000
Waimakariri (New Zealand)	-7.62	-5.28	-15.94	Taylor and Fox, 1996
Patagonian Rivers				Brunet et al., 2005
Colorado	-4	-2.9	-4.9	
Negro	-5.49	-4.3	-6.3	
Chubut	-7.34	-5.7	-10	
Deseado	-6.32	-1.8	-9.8	
Chico	-4.56	-1.8	-8.8	
Santa Cruz	-4.25	-2.5	-5.5	
Coyle	-7.97	-5	-12.8	
Gallegos	-6.98	-5.5	-11.1	
Sugar Creek (USA)	-6.5	-5	-8	Tobias and Böhlke, 2011
Upper Green River-Greensburg	-12.31	-6.5	-15.24	**This Study**
Upper Green River-Munfordville	-12.21	-4.09	-17.68	

Source: Modified from Brunet et al. (2009).

Factors Influencing $\delta^{13}C_{DIC}$

Riverine DIC is influenced by a number of internal and external processes including soil respiration, carbonate mineral dissolution/precipitation, water-atmosphere exchange of gases, photosynthesis/respiration within the river and precipitation (Fig. 2-11). Of these sources, precipitation is often negligible (Tellmer and Viezer, 1999). The temperate climate of this study area, in combination with the variable geology, provided a unique insight into whole system carbon dynamics. Each source of carbon reacted to

seasonal shifts in different magnitudes and directions, thus making for a complex carbon cycling regime.

Soil Respiration and $\delta^{13}C_{DIC}$

Soil pCO_2 is a function of soil respiration and mineral weathering (Tellmer and Veizer, 1999). Soil respiration increases pCO_2 concentrations, which in turn lowers pH and dissolves minerals (Eq. 1-1). As minerals dissolve, pCO_2 is lowered as it is absorbed by the reaction, which raises the pH and converts carbonic acid to bicarbonate.

A large control on these two reactions is soil thickness and mineral weathering rates. Karst terrains have a characteristically thin soil, which limits their soil respiration levels, while silicate basins tend to have thicker soils allowing for increased respiration (Tellmer and Veizer, 1999). Silicates are far more resistant to chemical weathering compare to carbonate minerals and, as such, do not remove CO_2 from the soil as quickly. This caused the pCO_2 to be increased and pH to decrease in the upstream basin, as seen in Figure 2-5 A. The downstream, more carbonate rich, basin contains lower respiration levels and more buffered pH (Fig. 2-5 B).

Soil respired CO_2 was the main influence on the river $\delta^{13}C_{DIC}$ values in both the upstream and downstream catchments (Fig. 2-8, 2-9). Soil derived $\delta^{13}C_{DIC}$ is in equilibrium with vegetation respired CO_2 consistent with the C_3 pathway. The average soil $\delta^{13}C_{DIC}$ is –21‰ to –22‰, which was in agreement with established values for C_3 photosynthetic plants after taking into account molecular diffusion (Cerling et al., 1991; Clark and Fritz, 1995). At both sites, soil respired CO_2 had a seasonal trend with decreasing values from late fall/winter into the early spring. As photosynthesis

decreased during the winter, soil respiration produced less CO_2 allowing soil water to more closely mimic the $\delta^{13}C_{DIC}$ of precipitation in equilibrium with atmospheric CO_2 (Górka et al., 2011). Come spring, when photosynthesis increased, soil respiration fractionates the CO_2 yielding a depleted signal closer to –27‰ (Clark and Fritz, 1995), as seen at both sites.

This study found, with the exception of spring 2014, no relationships between pH and $\delta^{13}C_{DIC}$ values at either site, contrary to Brunet et al. (2009), who found strong relationships between and pH and $\delta^{13}C_{DIC}$ (r^2=0.57). This difference in geochemical controls was likely a result of differences in basin geology, with Brunet et al. (2009) studying a purely siliciclastic basin consisting of granitoids and gneisses. The pH of the system is primarily controlled by the dissolution of the carbonate bedrock (Barth et al., 2003), which is directly influenced by the amount of recharge to the system. In the upstream reach of the river there was markedly less cladophora vegetation (a filamentous green algae), yielding a moderated influence on DIC in the river. From late spring to early fall, the composite signal of soil respiration, carbonate mineral reactions, and water-air gas exchanges masked the relationship between pH and $\delta^{13}C_{DIC}$. In late winter through early spring, when the soil respiration was minimal and dissolved CO_2 decreases to a minimum, the dissolution of carbonate minerals caused by early spring precipitation highlights the relationship. The relationship between pH and $\delta^{13}C_{DIC}$ values had a relatively strong correlation (r^2=0.42) until photosynthesis increased and the relationship diminished. During this transition from low photosynthetic activity and high precipitation to higher levels of photosynthesis, the mixing model predicted soil respiration to not be the primary source of DIC in the river. The more rapid response of

groundwater to early spring rains was evident beginning in April, 2014 (Fig. 2-10). Conversely, the more productive downstream reach continued to be controlled by soil respiration from aquatic and riparian vegetation (Fig. 2-9).

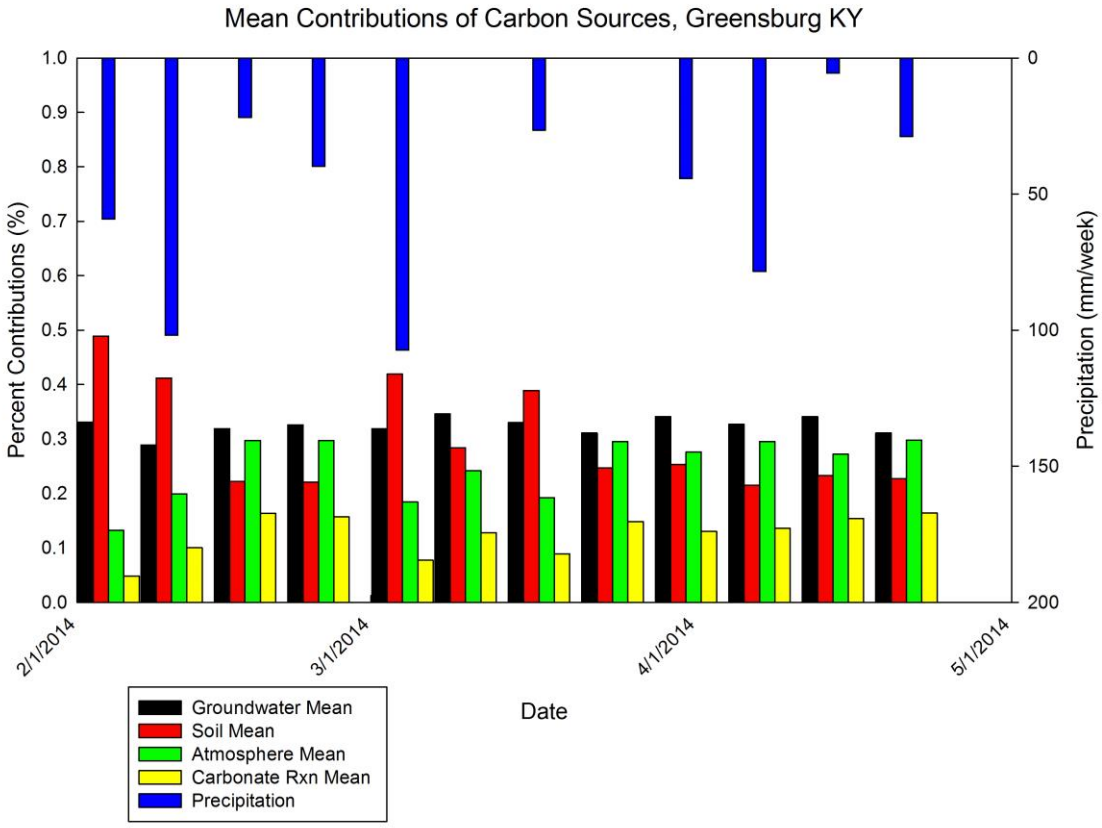

Fig. 2-10: Mixing model results for late winter/early spring in the upstream basin. Note the shift in primary carbon sourcing from soil respiration to groundwater in mid-March. Source: Created by the author.

Carbonate Mineral Dissolution controls on $\delta^{13}C_{DIC}$

Carbonate dissolution imparts a strong influence on river geochemistry with a strong pH buffering capacity and providing large quantities of DIC in the form of bicarbonate (Drever, 1982; Schulte et al., 2011). Due to the large (10‰) difference in $\delta^{13}C_{DIC}$ values between soil water and groundwater typically found in catchments, the

contribution of each is easily delineated (Doctor et al., 2008). Carbonate dissolution, mediated by acidified meteoric waters, provides half the DIC found in groundwater. The other half is likely a result of CO_2 dissolving into soil water (Amiotte-Suchet and Probst, 1995).

The enriched $\delta^{13}C_{DIC}$ values observed in the winter at the Green River sites were likely due to groundwater inputs bringing enriched DIC to the river from the weathering of carbonate bedrock (–12‰) (Spiro and Pentecost, 1991; Clark and Fritz, 1997; Mook and de Vries, 2000; de Montety et al., 2011). Streams undergoing a rapid gain in discharge through groundwater inputs show enriched $\delta^{13}C_{DIC}$ values (Atekwana and Krishnamurthy, 1998; Waldron et al., 2009; Tobias and Böhlke, 2011). In the early spring, when vegetation was still dormant, both basins showed enrichment (–10‰) of $\delta^{13}C_{DIC}$ commensurate with increased precipitation and enhanced carbonate weathering, which contributes a higher proportion of bicarbonate to the system. This is seen in the seasonal mixing model results when carbonate reaction contributions increase several percentage points and soil respiration decreases in its contribution.

Differences in basin geology typically contribute to differences in river $\delta^{13}C_{DIC}$ records; however, no difference was noted in this study. Even with less limestone in the upstream basin, there was still enough carbonate bedrock to strongly influence the overall $\delta^{13}C_{DIC}$ signal. The mixing model results demonstrate this with similar contributions from carbonate reactions from both basins (10-15%) (Tables 2-1, 2-2). Tellmer and Veizer (1999) studied several river basins in the Ottawa River system and determined relationships for DIC and $\delta^{13}C_{DIC}$ based on the basin geology (Fig. 2-11),

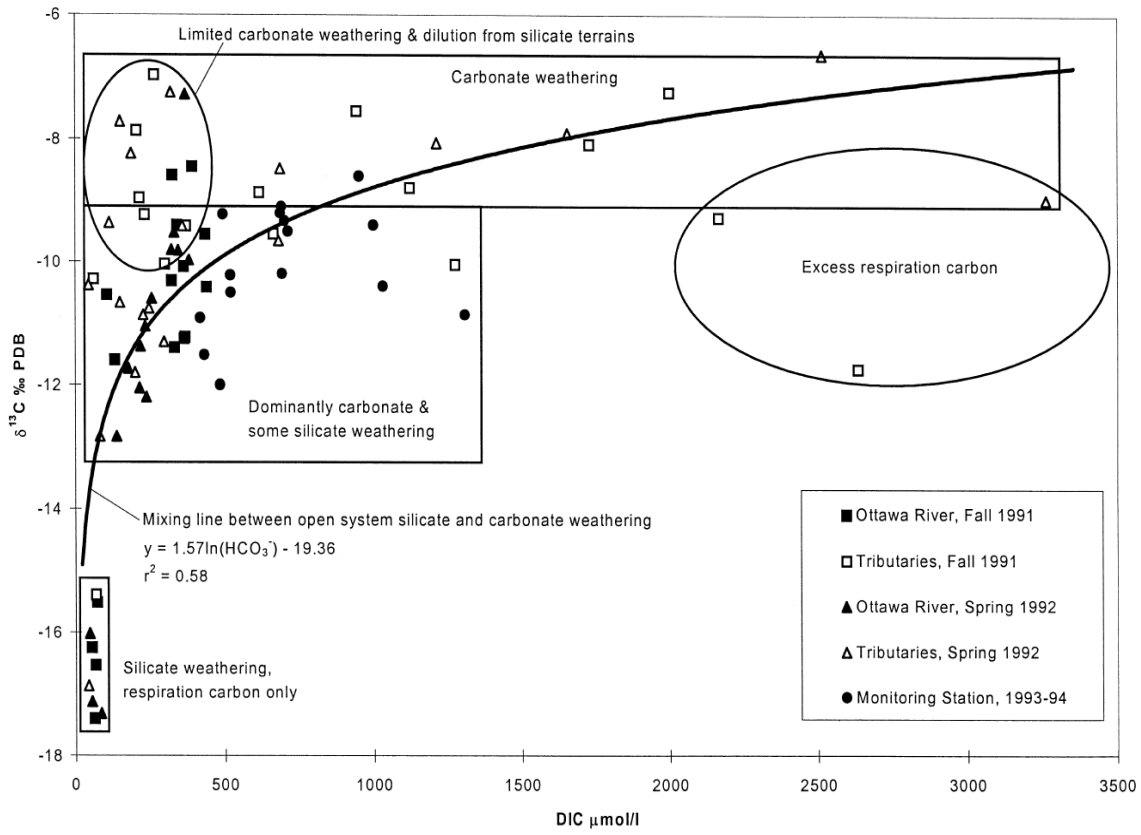

Fig. 2-11: Relationship between DIC and $\delta_{13}C$ from the Ottawa River basin. Note the relationships for pure silicate, mixed silicate/carbonate, and pure carbonate regimes. Source: Adapted from Tellmer and Veizer (1999).

finding differences between carbonate and siliciclastic basins.

Assuming similar relationships in the Green River basin, a difference should be noted between the upstream and downstream river signals as one was dominantly carbonate while the other a mixture with silicate and carbonate bedrock; however, no relationship existed in this study. Both basins, regardless of the underlying geology, maintained fairly constant $\delta^{13}C_{DIC}$ values throughout the year (both basins average –12.3‰) with minor fluctuations pertaining to vegetation and groundwater influences (Fig. 2-12). The enrichment normally expected with more carbonate weathering downstream was likely offset by increased plant productivity within the river, influences

from the dam, or mixing that creates homogeneity, or all the above.

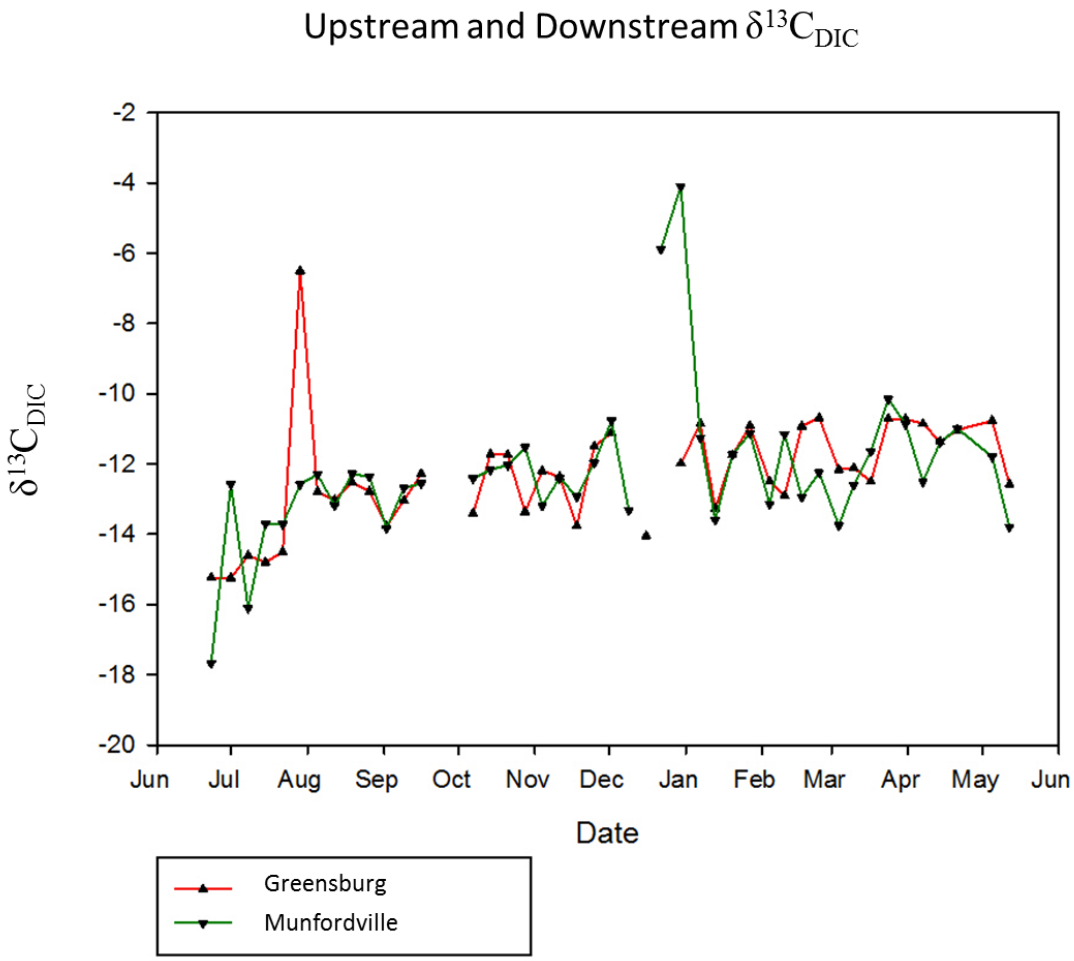

Fig. 2-12: Time series of river $\delta^{13}C_{DIC}$. Note the depleted values in fall 2013 and more enriched values in spring 2014. Source: Created by the author.

Water-Gas Exchange of CO_2

When the relative partial pressure of CO_2 in the river is higher than the surrounding atmosphere, CO_2 will readily degas from the stream (Doctor et al., 2008). As CO_2 degasses, kinetic fractionation of the carbon causes an enrichment of ~14.7‰ (Zhang et al., 1995). Typically, rivers have higher pCO_2 concentrations compared to the

atmosphere, so there is a steady decline in pCO_2 downriver (Schulte et al., 2011). An exception to this is when rivers are impounded by dams, like the Green River dam. In this case, the impoundment effectively can allow the water to degas all of its CO_2 until equilibrium is reached with respect to atmospheric pCO_2.

Yu et al. (2008) studied three reservoirs in China for carbon cycling trends over various depths. The $\delta^{13}C_{DIC}$ trend was found to be highly enriched approximately -4‰ to -6‰ at the surfaces of the reservoirs during the summer (Yu et al., 2008). This extremely enriched DIC was one explanation for the anomalous enriched sample (Greensburg 7/29/13) at –6.5‰. Coinciding with the enriched signal, the Green River Dam released an appreciable amount of water in late July-early August (Fig. 2-8). The $\delta^{13}C_{DIC}$ progressively depleted throughout the fall and winter until winter values reached approximately –8‰ to –10‰. This seasonal shift in reservoir $\delta^{13}C_{DIC}$ may also explain why wintertime DIC was enriched to –10‰ to –11‰ as reservoir water flushed through the system to combine with soil water already in equilibrium with atmospheric CO_2.

The upper Green River transitions from a mixture of siliciclastic and carbonate lithologies to one of almost pure limestone. When this happens, the inflow of soil and groundwater laced with higher pCO_2 concentrations will force CO_2 to dissolve into the river (Schulte et al., 2011). Herczeg and Fairbanks (1987) found that the resulting kinetic fractionation of dissolving CO_2 into the water is of a similar magnitude to degassing (-13‰). As pCO_2 increases throughout the river, the resulting drop in pH forces carbonate minerals to dissolve, thereby altering the particulate and dissolved inorganic carbon loadings (Drever, 1982).

2.6 Conclusions

This study investigated the effects of seasonality and varying lithologies on inorganic carbon cycling over the course of one year. Carbon sourcing showed distinct temporal and spatial patterns relating to changes in basin geology and vegetation differences. In both spatial and temporal frameworks, carbon chemistry was controlled by soil respiration, groundwater flux, air-water gas exchange, and carbonate reactions, in order of decreasing importance. The less carbonate-rich upstream basin clearly showed soil respiration contributes >30% of all DIC from late spring through winter. In the early spring, while vegetation was still inactive, heavy precipitation became the main source of DIC contributing upwards of 30% of total DIC. The downstream catchment is primarily influenced by soil respired DIC throughout the year likely due to more plant productivity within the river.

The lack of atmospheric contributions indicates that the river remained in equilibrium with atmospheric pCO_2 even with several large tributaries and karst springs. The carbonate aquifers in the upstream and downstream basin likely removed most CO_2 from groundwater by converting it to bicarbonate, thereby not allowing pCO_2 to shift from equilibrium within the river. A second conclusion is the degassed water exiting the Green River Reservoir was still in equilibrium until well past the Greensburg sampling site. By the time that water reached Munfordville, the mixing and dilution of river water with karst groundwater diminished any atmospheric exchange.

Despite the varying geology, the production of DIC from carbonate reactions appears no different between reaches/sites. Other studies have noted that even a small percentage of carbonate bedrock is enough to alter the carbon chemistry of a largely

siliciclastic basin. This study shows this trend to be accurate with both the upstream and downstream basins gaining approximately 10%-20% DIC from carbonate reactions

Given the high degree of control vegetation and groundwater have on DIC in the upper Green River, more work is needed to delineate DIC contributions and uptake of aquatic versus riparian vegetation over differing timescales. Understanding storm event influences on biogeochemical cycles is crucial to fully understanding the complex dynamics in large catchments. Future studies should aim to investigate large watersheds like the upper Green River at high temporal resolutions to capture and understand weekly, monthly, seasonal, and yearly carbon dynamics and better constrain the global carbon cycle.

CHAPTER THREE: CONCLUSIONS

This study set out to delineate the spatial and temporal controls on the upper Green River carbon cycle from June, 2013, through May, 2014, using stable carbon isotopes. While many studies have explored the riverine carbon cycle around the world, few studies exist that investigate large mid-latitude river systems with high degrees of karstification using carbon isotope sourcing. The geologic, vegetative, and hydrologic variables associated with this study helped answer several important questions regarding seasonal carbon cycling and have led to asking several more.

There were dynamic seasonal shifts in carbon sourcing from soil respiration and groundwater fluxes. There was an overall depletion of $\delta^{13}C_{DIC}$ from soil respiration in the summer related to increased riparian and aquatic vegetation, while the winter was characterized by carbonate weathering-induced enrichment. While the bulk of DIC originated from soil respiration from late spring to winter, the early spring was characterized by heavy precipitation bringing the majority of DIC as ^{13}C enriched groundwater. It was found that carbonate reactions and atmosphere-water gas reactions contribute approximately 40% of all DIC to the system throughout the year and regardless of the underlying geology. This implies the small percentage of carbonate rock in the upstream basin is influential enough to overprint a dominantly siliciclastic basin.

While investigating the dynamics and complications of carbon cycling over a varying geologic landscape, insights were gained not only in the realm of natural carbon dynamics, but also in the anthropogenic realm. The Green River Dam provided a rare opportunity to study the natural response to anthropogenic activities over two different

watersheds. With the U.S. Army Corp of Engineers (USACE, 2011) recently stating interest in removing several lock and dam structures on the Green River, these data will provide key information regarding natural riverine responses to anthropogenic impoundments. The upper Green River is known for its biodiversity and productivity, thus making it an excellent platform to study both aquatic and riparian vegetation biogeochemical cycles further. This study is one small component in understanding and quantifying the global carbon cycle and specifically the carbon fluxes through karst watersheds.

APPENDIX 1: RAW ISOTOPE DATA SAMPLE

	1-Date	2-GB River-Time	3-GB River-pH	4-GB River-SpC	5-GB River-Temp	6-GB River13C	GB River-13C Std	8	GB Precip-Averag	GB Precip-Media	11	12	13-GB Well-time	14-GB Well-pH	15-GB Well-SpC	16-GB Well-temp	17-GB Well-13C	GB Well-13C std	19
1	6/22/2013	955.0000	7.4300	145.0000	24.8000	-15.2346	0.0343		1.7867	1.2400	31.4960								
2	7/1/2013	1115.0000	7.2700	140.0000	21.0700	-15.2430	0.0568		1.2133	0.6400	16.2560								
3	7/8/2013	1018.0000	7.6700	303.0000	8.5400	-14.6070	0.0461		7.3400	6.1900	157.2260								
4	7/15/2013	1127.0000	6.6400	173.3000	27.6000	-14.8034	0.0321		0.8067	0.7400	18.7950								
5	7/22/2013	1030.0000	6.4700		23.2000	-14.5028	0.0312		0.7900	0.5400	13.7160								
6	7/29/2013	1109.0000	6.4500	182.7000	24.0000	-6.5020	0.0386		1.4267	1.4600	37.0840		1032.0000	6.4700	310.7000	21.9000	-11.6468	0.1129	
7	8/5/2013	1054.0000	6.9200	153.0000	24.4600	-12.7948	0.0413		0.9233	1.0700	27.1780		1020.0000	6.7800	355.0000	18.8300	-11.6458	0.1488	
8	8/12/2013	1108.0000	7.3500	178.0000	25.3100	-13.0216	0.0627		1.7633	1.5000	38.1000		1037.0000	6.9100	370.0000	21.1300	-11.1844	1.2636	
9	8/19/2013					-12.5290	0.0123		1.7133	1.3600	34.5440						-11.4054	0.0858	
10	8/26/2013	1152.0000	7.0600	159.0000	26.4700	-12.7800	0.0402		0.0767	0.0400	1.0160		1129.0000	7.1400	393.0000	20.0600	-11.4814	0.1179	
11	9/2/2013	1014.0000	7.0600	182.0000	23.8400	-13.7628	0.0225		2.6700	2.9000	73.6600		931.0000	6.2800	388.0000	19.1200	-11.7272	0.2079	
12	9/9/2013	1033.0000	7.0100	147.0000	25.4300	-13.0396	0.0367		0.0500	0.0300	0.7620		1004.0000	6.7200	345.0000	19.0400	-11.6884	0.1617	
13	9/16/2013	1038.0000	6.8900	197.0000	20.8400	-12.2842	0.0432		0.2833	0.0900	2.2860		1001.0000	6.6400	390.0000	18.4900	-11.5736	0.0138	
14	9/23/2013	1059.0000	7.0800	169.0000	20.2900						--		1028.0000	6.3200	399.0000	17.1600			
15	9/30/2013	1010.0000	7.1800	147.0000	20.7500						--		907.0000	5.9800	369.0000	17.0200			
16	10/7/2013	1140.0000	7.2400	98.0000	19.5500	-13.4103	0.0720		2.0100	1.9300	49.0220		1015.0000	6.0800	371.0000	17.0400	-11.9110	0.0283	
17	10/14/2013	1100.0000	7.1400	144.0000	18.7100	-11.7227	0.0595		0.0000	0.0000	0.0000		1000.0000	7.2000	355.0000	16.8000	-11.6064	0.0805	
18	10/21/2013	1030.0000	6.3700	151.0000	15.9600	-11.7409	0.0619		0.8500	0.8400	21.3360		952.0000	7.9700	366.0000	18.3200	-11.4484	0.0754	
19	10/28/2013	845.0000	6.3500	139.0000	13.1700	-13.3660	3.0957e-3		0.4467	0.3800	9.6520		816.0000	6.6400	306.0000	20.5800	-12.0875	8.5049e-3	
20	11/4/2013	1054.0000	6.3300	223.0000	14.5000	-12.1940	0.0481		1.5700	1.3100	33.2740		1010.0000	6.5300	371.0000	16.2700	-11.8261	0.2342	
21	11/11/2013	935.0000	5.5000	158.0000	12.3600	-12.3687	0.0399		0.7033	0.6800	17.2720		844.0000	6.2000	403.0000	15.3000	-11.8323	0.0136	
22	11/18/2013	1035.0000	7.0800	182.0000	16.2000	-13.7570	0.0345		2.3200	2.5100	63.7540		894.0000	7.0300	333.0000	18.4400	-11.6681	0.0409	
23	11/25/2013	955.0000	6.4500	126.0000	7.4600	-11.4937	0.0417		0.4667	0.4200	10.6680		915.0000	6.8300	314.0000	18.1000	-11.7192	0.0233	
24	12/2/2013	1026.0000	6.3400	195.0000	10.3800	-11.1158	0.0397		0.8700	0.4900	12.4460		946.0000	7.2500	3.6400	15.9500	-11.7785	0.0320	
25	12/9/2013	1215.0000	5.5700	184.0000	6.4000						--		1125.0000	6.1700	475.0000	13.6000			
26	12/16/2013	1015.0000		125.0000	6.4300	-14.0503	0.0216		0.6500	0.6000	15.2400		935.0000	6.3600	339.0000	15.7800			
27	12/22/2013	845.0000	6.4200	203.0000	11.7700						--		1000.0000	6.4700	4.3700	14.7900			
28	12/30/2013					-11.9855	0.1042		0.8567	0.8300	21.0820						-11.7313	0.0786	
29	1/7/2014	1244.0000		208.0000	0.3300	-10.8532	0.0694		2.4867	3.0400	77.2160								
30	1/13/2014	1000.0000	6.4000	170.0000	5.8300	-13.2703	0.0905		0.7800	0.8400	21.3360		930.0000	6.6500	398.0000	19.1000	-9.8386	0.0481	
31	1/20/2014	1000.0000	7.1800	133.0000	5.3000	-11.7371	0.1056		1.5700	1.0600	26.9240		1110.0000	7.1700	349.0000	18.1000	-9.9670	0.0405	
32	1/27/2014	1000.0000		177.0000	2.2500	-10.9169	0.1089		4.3367	4.0700	103.3780		922.0000	6.4600	373.0000	9.0800	-10.2571	0.0559	
33	2/4/2014	1510.0000	5.8700	158.0000	4.2100	-12.4983	0.0665		2.3033	2.3300	59.1820		1430.0000	6.5600	355.0000	14.1300	-10.5057	0.0573	
34	2/10/2014	922.0000	5.6600	159.0000	1.0400	-12.9007	0.0516		4.3867	4.0100	101.8540								
35	2/17/2014	1020.0000	6.6600	159.0000	4.9300	-10.9247	0.0565		0.9433	0.8600	21.8440		145.0000	6.8600	392.0000	20.2300	-10.6529	0.0478	
36	2/24/2014	935.0000	6.7800	133.0000	4.2900	-10.6902	0.1077		1.5367	1.5700	39.8780								
37	3/4/2014	1321.0000	6.3400	189.0000	4.4800	-12.1575	0.0961		5.0817	4.2250	107.3150								
38	3/10/2014	11.4800	5.9000	119.0000	10.0200	-12.1111	0.1026		0.3667	0.0000	0.0000		1224.0000	6.6300	326.0000	18.8400	-10.6628	0.0796	
39	3/17/2014	109.0000	7.2000	104.0000	4.6500	-12.5012	0.0499		1.0383	1.0450	26.5430		1130.0000	7.1100	264.0000	13.1800	-10.4739	0.0555	
40	3/24/2014	1420.0000	7.6100	140.0000	10.2700	-10.7092	0.0607		0.0000	0.0000	0.0000		1345.0000	6.6600	295.0000	27.7800	-10.7377	0.0372	
41	3/31/2014	1454.0000	7.3800	259.0000	13.2200	-10.7209	0.1129		1.7917	1.7450	44.3230		1422.0000	6.7800	379.0000	15.5400	-9.5187	0.0656	
42	4/7/2014	1033.0000	6.4600	239.0000	11.3000	-10.8540	8.2209e-3		2.9200	3.0900	78.4860		945.0000	6.3000	423.0000	17.4400	-10.1235	0.0423	
43	4/14/2014	1325.0000	7.3700	106.0000	16.3000	-11.3698	0.0193		0.2200	0.2200	5.5880		1246.0000	7.0400	296.0000	18.9500	-9.9303	0.0323	
44	4/21/2014	1010.0000	7.3400	167.0000	17.3500	-11.0308	0.0258		1.1350	1.1350	28.8290		1045.0000	6.8700	377.0000	19.8400	-11.1918	0.0572	

APPENDIX II: SAMPLE FIELD SHEET DATA

	1-Date	2-GB River-Time	3-GB River-pH	4-GB River-SpC	5-GB River-Temp	6-GB River-13C	GB River-13C Std	8	GB Precip-Averag	GB Precip-Media	11	12	13-GB Well-time	14-GB Well-pH	15-GB Well-SpC	16-GB Well-temp	17-GB Well-13C	GB Well-13C std	19
1	6/23/2013	955.0000	7.4300	145.0000	24.8000	-15.2346	0.0343		1.7867	1.2400	31.4960								
2	7/1/2013	1115.0000	7.2700	140.0000	21.0700	-15.2430	0.0568		1.2133	0.6400	16.2560								
3	7/8/2013	1018.0000	7.6700	303.0000	8.5400	-14.6070	0.0461		7.3400	6.1900	157.2260								
4	7/15/2013	1127.0000	6.6400	173.3000	27.6000	-14.8034	0.0321		0.8067	0.7400	18.7960								
5	7/22/2013	1030.0000	6.4700		23.2000	-14.5028	0.0312		0.7900	0.5400	13.7160								
6	7/29/2013	1109.0000	6.4500	182.7000	24.0000	-6.5020	0.0386		1.4267	1.4600	37.0840		1032.0000	6.4700	310.7000	21.9000	-11.6468	0.1129	
7	8/5/2013	1054.0000	6.9200	153.0000	24.4600	-12.7948	0.0413		0.9233	1.0700	27.1780		1020.0000	6.7800	355.0000	18.8300	-11.6458	0.1488	
8	8/12/2013	1108.0000	7.3500	178.0000	25.3100	-13.0216	0.0627		1.7633	1.5000	38.1000		1037.0000	6.9100	370.0000	21.1300	-11.1844	1.2636	
9	8/19/2013					-12.5290	0.0123		1.7133	1.3600	34.5440						-11.4054	0.0858	
10	8/26/2013	1152.0000	7.0600	159.0000	26.4700	-12.7800	0.0402		0.0767	0.0400	1.0160		1129.0000	7.1400	393.0000	20.0600	-11.4814	0.1179	
11	9/2/2013	1014.0000	7.0600	182.0000	23.8400	-13.7628	0.0225		2.6700	2.9000	73.6600		931.0000	6.2800	388.0000	19.1200	-11.7272	0.2079	
12	9/9/2013	1033.0000	7.0100	147.0000	25.4300	-13.0396	0.0367		0.0500	0.0300	0.7620		1004.0000	6.7200	345.0000	19.0400	-11.6884	0.1617	
13	9/16/2013	1038.0000	6.8900	197.0000	20.8400	-12.2842	0.0432		0.2833	0.0900	2.2860		1001.0000	6.6400	390.0000	18.4900	-11.5736	0.0138	
14	9/23/2013	1059.0000	7.0800	169.0000	20.2900						--		1028.0000	6.3200	359.0000	17.1600			
15	9/30/2013	1010.0000	7.1800	147.0000	20.7500						--		907.0000	5.9800	369.0000	17.0200			
16	10/7/2013	1140.0000	7.2400	98.0000	19.5500	-13.4103	0.0720		2.0100	1.9300	49.0220		1015.0000	6.0800	371.0000	17.0400	-11.9110	0.0283	
17	10/14/2013	1100.0000	7.1400	144.0000	18.7100	-11.7227	0.0595		0.0000	0.0000	0.0000		1000.0000	7.2000	355.0000	16.8000	-11.6064	0.0805	
18	10/21/2013	1030.0000	6.3700	151.0000	15.9600	-11.7409	0.0619		0.8500	0.8400	21.3360		952.0000	7.9700	366.0000	18.3200	-11.4484	0.0754	
19	10/28/2013	845.0000	6.3500	139.0000	13.1700	-13.3660	3.0957e-3		0.4467	0.3800	9.6520		816.0000	6.6400	306.0000	20.5800	-12.0875	8.5049e-3	
20	11/4/2013	1054.0000	6.3300	223.0000	14.5000	-12.1940	0.0481		1.5700	1.3100	33.2740		1010.0000	6.5300	371.0000	16.2700	-11.8261	0.2342	
21	11/11/2013	935.0000	5.5000	158.0000	12.3600	-12.3687	0.0399		0.7033	0.6800	17.2720		844.0000	6.2000	403.0000	15.3000	-11.8323	0.0136	
22	11/18/2013	1035.0000	7.0800	182.0000	16.2000	-13.7570	0.0345		2.3200	2.5100	63.7540		894.0000	7.0300	333.0000	18.4400	-11.6681	0.0409	
23	11/25/2013	955.0000	6.4500	126.0000	7.4600	-11.4937	0.0417		0.4667	0.4200	10.6680		915.0000	6.8300	314.0000	18.1000	-11.7192	0.0233	
24	12/2/2013	1026.0000	6.3400	195.0000	10.3800	-11.1158	0.0397		0.8700	0.4900	12.4460		946.0000	7.2500	3.6400	15.9500	-11.7785	0.0320	
25	12/9/2013	1215.0000	5.5700	184.0000	6.4000						--		1125.0000	6.1700	475.0000	13.6000			
26	12/16/2013	1015.0000		125.0000	6.4300	-14.0503	0.0216		0.6500	0.6000	15.2400		935.0000	6.3600	339.0000	15.7800			
27	12/22/2013	845.0000	6.4200	203.0000	11.7700						--		1000.0000	6.4700	4.3700	14.7900			
28	12/30/2013					-11.9855	0.1042		0.8567	0.8300	21.0820						-11.7313	0.0786	
29	1/7/2014	1244.0000		208.0000	0.3300	-10.8532	0.0694		2.4867	3.0400	77.2160								
30	1/13/2014	1000.0000	6.4000	170.0000	5.8300	-13.2703	0.0905		0.7800	0.8400	21.3360		930.0000	6.6500	398.0000	19.1000	-9.8386	0.0481	
31	1/20/2014	1000.0000	7.1800	133.0000	5.3000	-11.7371	0.1056		1.5700	1.0600	26.9240		1110.0000	7.1700	349.0000	18.1000	-9.9670	0.0405	
32	1/27/2014	1000.0000		177.0000	2.2500	-10.9169	0.1089		4.3367	4.0700	103.3780		922.0000	6.4600	373.0000	9.0800	-10.2571	0.0559	
33	2/4/2014	1510.0000	5.8700	158.0000	4.2100	-12.4983	0.0665		2.3033	2.3300	59.1820		1430.0000	6.5600	355.0000	14.1300	-10.5057	0.0573	
34	2/10/2014	922.0000	5.6600	159.0000	1.0400	-12.9007	0.0516		4.3867	4.0100	101.8540								
35	2/17/2014	1020.0000	6.6600	159.0000	4.9300	-10.9247	0.0565		0.9433	0.8600	21.8440		145.0000	6.8600	392.0000	20.2300	-10.6529	0.0478	
36	2/24/2014	935.0000	6.7800	133.0000	4.2900	-10.6902	0.1077		1.5367	1.5700	39.8780								
37	3/4/2014	1321.0000	6.3400	189.0000	4.4800	-12.1575	0.0961		5.0817	4.2250	107.3150								
38	3/10/2014	11.4800	5.9000	119.0000	10.0200	-12.1111	0.1026		0.3667	0.0000	0.0000		1224.0000	6.6300	326.0000	18.8400	-10.6628	0.0796	
39	3/17/2014	109.0000	7.2000	104.0000	4.6500	-12.5012	0.0499		1.0383	1.0450	26.5430		1130.0000	7.1100	264.0000	13.1800	-10.4739	0.0555	
40	3/24/2014	1420.0000	7.6100	140.0000	10.2700	-10.7092	0.0607		0.0000	0.0000	0.0000		1345.0000	6.6600	295.0000	27.7800	-10.7377	0.0372	
41	3/31/2014	1454.0000	7.3800	259.0000	13.2200	-10.7209	0.1129		1.7917	1.7450	44.3230		1422.0000	6.7800	379.0000	15.5400	-9.5187	0.0656	
42	4/7/2014	1033.0000	6.4600	239.0000	11.3000	-10.8540	8.2209e-3		2.9200	3.0900	78.4860		945.0000	6.3000	423.0000	17.4400	-10.1235	0.0423	
43	4/14/2014	1325.0000	7.3700	106.0000	16.3000	-11.3698	0.0193		0.2200	0.2200	5.5880		1246.0000	7.0400	296.0000	18.9500	-9.9303	0.0323	
44	4/21/2014	1010.0000	7.3400	167.0000	17.3500	-11.0308	0.0258		1.1350	1.1350	28.8290		1045.0000	6.8700	377.0000	19.8400	-11.1918	0.0572	

APPENDIX III: GREENSBURG MIXING MODEL RESULTS

		Relative Contributions by Source															
		Groundwater				Soil				Atmosphere				Carbonate Reactions			
Mixture Date	N Value	Mean	Min	Max	Std	Mean	Min	Max	Std	Mean	Min	Max	Std	Mean	Min	Max	Std
9/16/2013	1651	29.60%	0.00%	88.00%	12.10%	39.90%	12.00%	70.00%	21.30%	20.80%	0.00%	62.00%	15.00%	9.70%	0.00%	30.00%	7.20%
10/7/2013	1094	24.90%	0.00%	74.00%	18.00%	50.90%	26.00%	76.00%	10.50%	16.40%	0.00%	49.00%	12.00%	7.80%	0.00%	24.00%	5.80%
10/14/2013	2082	33.10%	0.00%	98.00%	23.70%	35.20%	2.00%	70.00%	14.20%	21.90%	0.00%	65.00%	15.80%	9.80%	0.00%	30.00%	7.30%
10/21/2013	1957	32.20%	0.00%	96.00%	23.10%	33.60%	4.00%	66.00%	12.90%	23.10%	0.00%	69.00%	16.70%	11.20%	0.00%	34.00%	0.08%
10/28/2013	1233	26.90%	0.00%	80.00%	19.30%	46.40%	20.00%	73.00%	11.00%	17.90%	0.00%	53.00%	12.90%	8.80%	0.00%	27.00%	6.60%
11/4/2013	1800	32.00%	0.00%	95.00%	23.00%	32.90%	5.00%	62.00%	12.30%	23.00%	0.00%	69.00%	16.70%	12.00%	0.00%	36.00%	8.90%
11/11/2013	1711	31.20%	0.00%	93.00%	22.40%	34.60%	7.00%	64.00%	12.00%	22.50%	0.00%	67.00%	16.30%	11.70%	0.00%	35.00%	8.60%
11/18/2013	1123	25.00%	0.00%	74.00%	18.00%	46.20%	26.00%	69.00%	9.20%	18.80%	0.00%	56.00%	13.60%	10.00%	0.00%	30.00%	7.40%
11/25/2013																	
12/2/2013																	
12/9/2013	2117	34.20%	0.00%	98.00%	24.40%	26.90%	0.00%	59.00%	13.00%	25.60%	0.00%	76.00%	18.30%	13.40%	0.00%	40.00%	9.70%
12/16/2013	1064	25.10%	0.00%	75.00%	18.20%	45.50%	25.00%	68.00%	9.20%	18.70%	0.00%	56.00%	13.60%	10.70%	0.00%	31.00%	7.70%
12/30/2013	1841	32.60%	0.00%	97.00%	23.40%	29.10%	3.00%	59.00%	11.70%	24.70%	0.00%	74.00%	17.80%	13.50%	0.00%	41.00%	9.90%
1/7/2014	2195	33.40%	0.00%	93.00%	23.20%	20.90%	0.00%	52.00%	12.00%	29.30%	0.00%	84.00%	20.30%	16.40%	0.00%	47.00%	11.20%
1/13/2014	732	20.50%	0.00%	60.00%	14.70%	63.40%	40.00%	85.00%	9.70%	11.60%	0.00%	35.00%	8.50%	4.50%	0.00%	14.00%	3.60%
1/20/2014	2042	34.90%	0.00%	99.00%	24.90%	38.80%	0.00%	77.00%	17.00%	18.90%	0.00%	56.00%	13.60%	7.40%	0.00%	22.00%	5.50%
1/27/2014	2695	34.20%	0.00%	90.00%	22.60%	30.00%	0.00%	73.00%	17.30%	25.50%	0.00%	68.00%	17.00%	10.30%	0.00%	26.00%	6.30%
2/4/2014	1407	33.10%	0.00%	98.00%	23.80%	48.90%	2.00%	85.00%	17.80%	13.20%	0.00%	40.00%	9.70%	4.80%	0.00%	15.00%	3.70%
2/10/2014	1452	28.90%	0.00%	86.00%	20.80%	41.20%	14.00%	69.00%	11.50%	19.90%	0.00%	60.00%	14.50%	10.00%	0.00%	30.00%	7.40%
2/17/2014	2286	31.90%	0.00%	87.00%	21.50%	22.20%	0.00%	57.00%	13.30%	29.70%	0.00%	81.00%	20.00%	16.30%	0.00%	43.00%	10.00%
2/24/2014	2386	32.60%	0.00%	90.00%	22.20%	22.10%	0.00%	57.00%	13.20%	29.70%	0.00%	83.00%	20.20%	15.70%	0.00%	43.00%	10.00%
3/4/2014	1733	31.90%	0.00%	95.00%	22.90%	41.90%	5.00%	76.00%	14.90%	18.40%	0.00%	55.00%	13.40%	7.70%	0.00%	24.00%	5.80%
3/10/2014	1987	34.60%	0.00%	96.00%	24.40%	28.40%	0.00%	61.00%	13.70%	24.20%	0.00%	71.00%	17.10%	12.80%	0.00%	38.00%	9.20%
3/17/2014	1734	33.00%	0.00%	98.00%	23.70%	38.90%	2.00%	73.00%	14.90%	19.20%	0.00%	57.00%	14.00%	8.90%	0.00%	27.00%	6.60%
3/24/2014	2540	31.10%	0.00%	85.00%	20.70%	24.70%	0.00%	64.00%	15.10%	29.50%	0.00%	78.00%	19.90%	14.80%	0.00%	36.00%	8.50%
3/31/2014	2548	34.10%	0.00%	94.00%	23.50%	25.30%	0.00%	62.00%	14.30%	27.60%	0.00%	79.00%	19.10%	13.00%	0.00%	37.00%	8.80%
4/7/2014	2253	32.70%	0.00%	90.00%	22.40%	21.50%	0.00%	55.00%	12.60%	29.50%	0.00%	83.00%	20.20%	13.60%	0.00%	45.00%	10.60%
4/14/2014	2070	34.10%	0.00%	96.00%	24.10%	23.30%	0.00%	54.00%	12.10%	27.20%	0.00%	80.00%	19.20%	15.40%	0.00%	45.00%	10.90%
4/21/2014	2270	31.10%	0.00%	84.00%	20.80%	22.70%	0.00%	58.00%	13.70%	29.80%	0.00%	80.00%	19.90%	16.40%	0.00%	41.00%	9.90%

APPENDIX IV: MUNFORDVILLE MIXING MODEL RESULTS

		Relative Contributions by Source																	
		Groundwater				Soil				Atmosphere				Bedrock (carbonate minerals)					
Mixture Date	N Value	Mean	Min	Max	Std	Mean	Min	Max	Std	Mean	Min	Max		Mean	Min	Max	Std		
10/14/2013	1213	22.30%	0.00%	64.00%	16.10%	47.20%	36.00%	69.00%	8.00%	20.60%	0.00%	63.00%	14.90%	10.00%	0.00%	30.00%	7.50%		
10/21/2013	1289	23.10%	0.00%	69.00%	16.70%	37.30%	25.00%	56.00%	7.10%	25.40%	0.00%	75.00%	18.20%	14.20%	0.00%	42.00%	10.40%		
10/28/2013	1461	24.90%	0.00%	74.00%	17.90%	33.40%	20.00%	54.00%	7.60%	26.20%	0.00%	80.00%	19.20%	15.10%	0.00%	45.00%	11.00%		
11/4/2013	1025	20.90%	0.00%	62.00%	15.10%	43.90%	33.00%	61.00%	6.30%	22.40%	0.00%	67.00%	16.20%	12.80%	0.00%	39.00%	9.40%		
11/11/2013	1340	25.30%	0.00%	75.00%	18.20%	36.00%	25.00%	57.00%	7.60%	24.50%	0.00%	72.00%	17.80%	14.20%	0.00%	43.00%	10.40%		
11/18/2013	1279	25.50%	0.00%	76.00%	18.30%	38.10%	24.00%	60.00%	8.00%	23.20%	0.00%	69.00%	16.80%	13.20%	0.00%	40.00%	9.70%		
11/25/2013																			
12/2/2013	1707	24.00%	0.00%	72.00%	17.30%	36.40%	20.00%	61.00%	9.10%	26.80%	0.00%	80.00%	19.30%	12.80%	0.00%	39.00%	9.40%		
12/16/2013																			
12/22/2013	1127	21.80%	0.00%	65.00%	15.80%	9.60%	0.00%	29.00%	7.20%	22.00%	0.00%	65.00%	15.70%	46.60%	35.00%	71.00%	8.90%		
12/30/2013	585	15.50%	0.00%	46.00%	11.40%	6.80%	0.00%	21.00%	5.20%	15.20%	0.00%	45.00%	10.90%	62.50%	54.00%	79.00%	6.10%		
1/7/2014																			
1/13/2014	912	19.60%	0.00%	58.00%	14.20%	46.70%	36.00%	62.00%	5.90%	21.40%	0.00%	64.00%	15.50%	12.30%	0.00%	37.00%	9.10%		
1/20/2014	1354	22.60%	0.00%	67.00%	16.40%	39.30%	26.00%	60.00%	7.60%	25.00%	0.00%	74.00%	18.00%	13.10%	0.00%	40.00%	9.60%		
1/27/2014																			
2/4/2014																			
2/10/2014																			
2/17/2014																			
2/24/2014																			
3/4/2014																			
3/10/2014																			
3/17/2014																			
3/24/2014																			
3/31/2014																			
4/7/2014																			
4/14/2014																			
4/21/2014																			
5/5/2014	1374	25.10%	0.00%	75.00%	18.10%	32.00%	20.00%	51.00%	7.10%	26.80%	0.00%	80.00%	19.30%	16.10%	0.00%	48.00%	11.70%		
5/12/2014	929	20.60%	0.00%	60.00%	14.90%	44.20%	34.00%	60.00%	5.80%	22.00%	0.00%	66.00%	14.90%	13.20%	0.00%	40.00%	9.70%		

REFERENCES

Andres, R.J., Felding, D.J., Marland, G., Boden, T.A., Kumar, N., 1999. Carbon dioxide emissions from fossil-fuel use, 1751-1950. *Tellus* 51: 759-765.

Atekwana, E.A., Krishnamurthy, R.V., 1998. Seasonal variations of dissolved inorganic carbon and $\delta^{13}C$ of surface waters: application of a modified gas evolution technique. *Journal of Hydrology* 205: 265-278.

Amiotte-Suchet, P., Probst, J-L., 1993a. Modelling of atmospheric CO_2 consumption by chemical weathering of rocks: application to the Garonne, Congo, and Amazon basins. *Chemical Geology* 107: 205-210.

Amiotte-Suchet, P., Probst, J-L., 1993b. CO_2 consumed by chemical weathering of continents: influences of drainage and lithology. *Comptes Rendus de l'Académie des Sciences, Serie II: Sciences de la Terre et des Planètes* 317: 615-622.

Amiotte-Suchet, P., Probst, J-L., 1995. A global model for present day atmospheric CO_2 consumption by chemical erosion of continental rocks (GEM CO_2). *Tellus* 47B: 273-280.

Amiotte-Suchet, P., Probst, J-L., Ludwig, W., 2003. Worldwide distribution of continental rock lithology: Implications for the atmospheric/soil CO_2 uptake by continental weathering and alkalinity river transport to the oceans. *Global Biogeochemical Cycles* 17(2): DOI: 10.1029/2002GB001891.

Amiotte-Suchet, P., Aubert, P., Probst, D., Gauthier-Lafave, J-L., Viville, A., Andreux, D., 1999. $\delta^{13}C$ pattern of dissolved inorganic carbon in a small granitic catchments: the Strengbach case study Vosges mountains, France. *Chemical Geology* 159: 129-145.

Aucour, A.M., Sheppard, S.M., Guyomar, O., Wattelet, J., 1999. Use of ^{13}C to Trace origin and Cycling of Inorganic Carbon in the Rhône River System. *Chemical Geology* 259: 87-105.

Bade, D.L., Cole, J.J., 2006. Impact of chemically enhanced diffusion on dissolved inorganic carbon isotopes in a fertilized lake. *Journal of Geophysics Research*: *Oceans* 111(C1): DOI: 10.1029/2004JC002684.

Barnett, T.T., Pierce, D.W., Schnur, D., 2001. Detection of anthropogenic climate change in the world's oceans. *Science* 292: 270-274.

Barth J.A., Veizer, J., 1999. Carbon cycle in St. Lawrence aquatic ecosystems at wornwall (Ontario), seasonal and spatial variations. *Chemical Geology* 158: 107-128.

Barth, J.A., Veizer, J., Mayer, B., 1998. Origin of particulate organic carbon in the Upper St. Lawrence: isotopic constraints. *Earth and Planetary Science Letters* 162: 111-121.

Barth, J.A., Cronin, A.A., Dunlop, J., Kalin, R.M., 2003. Influence of carbonates on the riverine carbon cycle in an anthropogenically dominated catchment basin: evidence from major elements and stable isotopes in the Lagan River (N Ireland). *Chemical Geology* 200: 203-216.

Benke, A.C., Cushing, C.E., 2005. *Rivers of North America*. Toronto, Canada: Elsevier Inc.

Berner, R.A., 1989. Biogeochemical cycles of carbon and sulfur and their effect on atmosphere oxygen over Phanerozoic time. *Palaeogeography, Palaeoclimatology, Palaeoecology* 75: 97-122.

Bigeleisen, J., Mayer, M.G., 1947. Calculation of equilibrium constants for isotopic exchange reactions. *Journal of Chemical Physics* 15: 261-267.

Brunet, F., Dubois, K., Veizer, J., Ndondo, G.R.N., Ngoupayou, J.R.N., Boeglin, J.L., Probst, J-L., 2009. Terrestrial and fluvial carbon fluxes in a tropical watershed: Nyong basin, Cameroon. *Chemical Geology* 265: 563-572

Cerling, T.E., Solomon, D.K., Quade, J., Bowman, J.R., 1991. On the isotopic composition of carbon in soil carbon dioxide. *Geochimica et Cosmochimica Acta* 55: 3403–3405

Clark, I., Fritz, P., 1995. *Environmental isotopes in hydrogeology*. Boca Raton, FL: CRC Press LLC.

Cox, P.M., Betts, R.A., Jones, C.D., Spall, S.A., Totterdell, I.J., 2000. Acceleration of global warming due to carbon-cycle feedbacks in a coupled climate model. *Nature* 408: 184-187

Crowther, J., 1983. Carbon dioxide concentrations in some tropical karst soils, West Malaysia. *Catena* 10: 27-39

Das, A., Krishnaswami, S., Bhattacharya, S.K., 2005. Carbon isotope ratio of dissolved inorganic carbon (DIC) in rivers draining the Deccan Traps: sources of DIC and their magnitudes. *Earth and Planetary Science Letters* 236: 419-429

Davidson, E.A., Figueiredo, R.O., Markewitz, D., Afdenkampe, A.K.., 2010. Dissolved CO_2 in small catchment streams of eastern Amazonia: A minor pathway of terrestrial carbon loss. *Journal of Geophysical Research-Biogeosciences* 115(G4): DOI: 10.1029/2009JG001202.

Daoxian, Y., Zaihua, L., 1998. *Global karst correlation*. New York, NY: Science Press.

Degens, E., Kempe, S., Ittokkot, V., 1984.Monitoring carbon in world rivers. *Environment* 26: 29-33

de Montety, V.J., Martin, M.J., Cohen, C., Foster, C., Kurz, M.J., 2011. Influence of diel biogeochemical cycles on carbonate equilibrium in a karst river. *Chemical Geology* 283: 31-43

del Giorgio, P.A., Williams, P., 2005. *The Global Significance of Respiration in Aquatic Systems*. Oxford, U.K.: Oxford University Press.

Dicken, S.N., 1935. Kentucky Karst Landscapes. *The Journal of Geology* 42: 708-728.

Doctor, D.H., Kendall, C., Sebestyen, S.D., Shanley, J.B., Ohte, N., Boyer, E.W., 2008. Carbon isotope fractionation of dissolved inorganic carbon (DIC) due to outgassing of carbon dioxide from a headwater stream. *Hydrological Processes* 22: 2410-2423.

Drever, J.I., 1982. *The Geochemistry of Natural Waters: Surface and Groundwater Environments*. New York, NY: Prentice Hall.

Dubois, K., Lee, D., Veizer, J., 2010. Isotopic constraints on alkalinity, dissolved organic carbon and atmospheric carbon dioxide fluxes in the Mississippi River. *Journal of Geophysical Research-Biogeosciences* 115(G2): DOI: 10.1029/2009JG001102.

Enting, I.G., Wigley, T.M.L., Heimann, M., 1994. *Future emissions and concentrations of carbon dioxide: key ocean/atmosphere/land analyses*. Canberra, Australia: CSIRO Division of Atmospheric Research Technical Paper 31

Esser, H.G., Carminati, A., Vontobel, P., Lehmann, E., Oswald, S.E., 2010. Neutron radiography and tomography of water distribution in the root zone. *Journal of Plant Nutrition and Soil Science* 173: 757–764

Fan, S., Gloor, M., Mahlman, S., Sarmiento, J., Takahashi, T., Tans, P., 1998. A Large Terrestrial Carbon Sink in North America Implied by Atmospheric and Oceanic Carbon Dioxide Data and Models. *Science* 282: 442-446

Fenneman, N.M., 1938. *Physiography of eastern United States*. New York, NY: McGraw-Hill.

Finlay, J.C., 2003. Controls of Streamwater Dissolved Inorganic Carbon Dynamics in a Forested Watershed. *Biogeochemistry* 62: 231-252

Flintrop, C., Hohlmann, B., Jasper, T., Korte, C., Podlaha, O.G., Scheele, S., Veizer, J., 1996. Anatomy of pollution: rivers of North Rhine-Westphalia, Germany. *American Journal of Science* 296: 58-98

Fonselius, S., Koroleff, F., Wärme, K-E., 1956. Carbon dioxide variations in the atmosphere. *Tellus* 8(2): 176-183.

Ford, D.C., Williams, P.W., 2007. *Karst hydrogeology and geomorphology*. Chichester, U.K.: John Wiley and Sons Ltd.

Friedlingstein, P., Prentice, I.C., 2010. Carbon-climate feedbacks: A review of model and observation based estimates. *Current Opinion in Environmental Sustainability* 2(4): 251-257.

Friedlingstein, P., Bopp, L., Ciais, P., Dufresne, J., Fairmont, L., LeTreut, H., Monfrey, P., Orr, J., 2001. Positive feedback between future climate change and the carbon cycle. *Geophysical Research Letters* 28: 1543-1546.

Friedlingstein, P., Dufresne, J.L., Cox, P.M., Rayner, P., 2003. How positive is the feedback between climate change and the carbon cycle? *Tellus* 55: 692-700.

Gonfiantini, R., Zuppi, G.M., 2003. Carbon isotope exchange rate of DIC in karst groundwater. *Chemical Geology* 197: 319-336.

Górka, M., Sauer, P.E., Lewicka-Szczebak, D., Jędrysek, M., 2011. Carbon isotope signature of dissolved inorganic carbon (DIC) in precipitation and atmospheric CO_2. *Environmental Pollution* 159: 294-301.

Hatcher, B.E., 2013. *Sources of CO_2 controlling the carbonate chemistry of the Logsdon River, Mammoth Cave, Kentucky*. M.S. in Geoscience, Department of Geography and Geology, Western Kentucky University. Online at: http://digitalcommons.wku.edu/theses/1311/.

Herczeg, T.E., Fairbanks, R.G., 1987. Anomalous carbon isotope fractionation between atmospheric CO_2 and dissolved inorganic carbon induced by intense photosynthesis. *Geochimica et Cosmochimica Acta* 51: 895-899.

Hess, J.W., 1974. *Hydrochemical investigations of the central Kentucky karst aquifer system*. Ph.D. Dissertation, The Pennsylvania State University, State College, Pennsylvania.

Hess, J.W., White, W.B., 1988. Storm water response of the karstic carbonate aquifer of southcentral Kentucky. *Journal of Hydrology* 99: 235-252.

Hitchon, B., Krouse, H.R., 1972. Hydrogeochemistry of the surface water of the Mackenzie River drainage basin, Canada—III. Stable isotopes of oxygen, carbon, and sulfur. *Geochimica et Cosmochimica Acta* 36: 1337-1357.

Hope, D., Palmer, S.M., Billett, M.F., Dawson, J.J.C., 2001. Carbon Dioxide and methane evasion from a temperate peatland Stream. *Limnol Oceanography* 46: 847-857.

IPCC (Intergovernmental Panel on Climate Change), 2007. *Climate Change 2007: The Scientific Basis. Contribution of Working Group I to the Fourth Assessment Report of the Intergovernmental Panel on Climate Change*. Solomon, S., D. Qin, M. Manning, Z. Chen, M. Marquis, K.B. Averyt, M. Tignor, H.L. Miller (eds.) New York, NY: Cambridge University Press.

Katz, B.G., Dehan, R.S., Hirten, J.J., Catches, J.S., 1997. Interactions between ground water and surface water in the Suwannee River basin, Florida. *Journal of the American Water Resources Association* 33: 1237-1254

KCC (Kentucky Climate Center), 2013. *Daily climate records*. Online at: http://www.kyclimate.org/climdata.html. Accessed March 14, 2013.

Keeling, C.D., Bacastow, R.B., Carter, A.F., Piper, S.C., Whorf, T.P., Heimann, M., Mook, W.G., Roeleffzen, H., 1989. *Aspects of Climate Variablility in the Pacific and Western Americas*. Washington, D.C.: American Geophysical Union, Geophysical Monograph 55.

Keeling, C.D., Piper, S.C., Bacastow, R.B., Wahlen, M., Whorf, T.P., Heimann, M., Meijer, H.A., 2005. Atmospheric CO_2 and $^{13}Co_2$ exchange with the terrestrial biosphere and oceans from 1978 to 2000: observations and carbon cycle implications. *Ecological Studies* 177: 83-113.

Keeling, C.D., Piper, S.C., Whorf, T.P., Keeling, R.F., 2011. Evolution of natural and anthropogenic fluxes of atmospheric CO_2 from 1957 to 2003. *Tellus* 63B: 1-22

KGRCREP (Kentucky Green River Conservation Reserve Enhancement Program), 2010. *Annual program accomplishment report. CEP-68R*. Frankfort, KY. Online at: http://www.apfo.usda.gov/Internet/FSA_File/crep2010annualreport.pdf.

Kininmonth, W., 2010. A natural constraint to anthropogenic global warming. *Energy and Environment* 21: 225-236.

Klimchouk, A.B., Ford, D.C., Palmer, A.N., Dreybrodt, W., 2000. *Speleogenesis: Evolution of Karst Aquifers*. Huntsville, AL: National Speleological Society.

Kling, G.W., Kipphut, G.W., Miller, M.C., 1992. The Flux of CO_2 and CH_4 from Lakes and Rivers in Arctic Alaska. *Hydrobiologica* 240: 23-46.

Lasaga, A.C., Soler, J.M., Ganor, J., Burch, T.E., Nagy, K.L., 1994. Chemical weathering rate laws and global geochemical cycles. *Geochimica et Cosmochimica Acta* 58: 2361-2386.

Lawhon, N., 2014. Investigating telogenetic karst aquifer processes and evolution in south-central Kentucky, U.S., using high-resolution storm hydrology and geochemical monitoring. M.S. in Geoscience, Department of Geography and Geology, Western Kentucky University. Online at: http://digitalcommons.wku.edu/theses/1324/.

Lean, J.L., Rind, D.H., 2008. How natural and anthropogenic influences alter global and regional surface temperatures: 1889 to 2006. *Geophysical Research Letters* 35(18): DOI: 10.1029/2008GL034864.

Le Cléré, C., Raupach, M.R., Canadell, J.G., Marland, G., Bopp, L., Ciais, P., Conway, T.J., Doney, S.C., Feely, R.A., Foster, P., Friedlingstein, P., Gurney, K., Houghton, R.A., House, J.I., Huntingford, C., Levy, P.E., Lomas, M.R., Majkut, J., Metzl, N., Ometto, J.P., Peters, G.P., Prentice, I.C., Randerson, J.T., Running, S.W., Sarmiento, J.L., Schuster, U., Sitch, S., Takahashi, T., Viovy, N., van der Werf, G.R., Woodward, F.I., 2009. Trends in the Sources and Sinks of Carbon Dioxide. *Nature Geoscience* 2: 831-836

Loáiciga, H.A., Maidment, D.R., Valdes, J.B., 2000. Climate-change impacts in a regional karst aquifer, Texas, USA. *Journal of Hydrology* 227: 173–194

Ludwig, W., Amiotte-Suchet, P., Probst, J-L., 1996a. River discharges of carbon to the world's ocean: determining local inputs of alkalinity and of dissolved and particular organic carbon. *Comptes Rendus de l'Academie des Sciences de Paris* 323: 1007–1014

Ludwig, W., Probst, J-L., Kempe, S., 1996b. Predicting the oceanic input of organic carbon by continental erosion. *Global Biogeochemical* 10: 21-41

Meybeck, M., 1987. Global chemical weathering of surficial rocks estimated from river dissolved loads. *American Journal of Science* 287: 401-428

Mook, W.G., de Vries, J.J., 2000. Environmental isotopes in the hydrological cycle-Principles and applications. *Technical Documents in Hydrology* 39. Online at: http://www.iup.uniheidelberg.de/institut/aktuelles/studium/lehre/AquaPhys/docPAS/IEHC_contents.pdf

Murphy, G.M., Urey, H.C., 1932. On the relative abundances of the nitrogen and oxygen isotopes. *Physical Review* 41(2): 141-148.

Nier, A.O., Gulbransen, E.A. 1939. Variations in the relative abundance of the carbon isotopes. *Journal of American Chemistry Society* 61: 697-698.

O'Driscoll, M.A., DeWalle, D.R., 2006. Stream-air temperature relations to classify stream-ground water interactions in a karst setting, central Pennsylvania, USA. *Journal of Hydrology* 329: 140-153

Osterhoudt, L.L., 2014. *Impacts of carbonate mineral weathering on hydrochemistry of the upper Green River basin, Kentucky*. M.S. in Geoscience, Department of Geography and Geology, Western Kentucky University. Online at: http://digitalcommons.wku.edu/theses/1337/.

Palmer, A.N., 1981. *A Geological Guide to Mammoth Cave National Park*. Dayton, OH: Cave Books.

Palmer, A.N., 2007. *Cave Geology*. Dayton, OH: Cave Books.

Palmer, A.N., Palmer, M.V. (eds.), 2009. Caves and Karst of the USA. Huntsville, AL: National Speleological Society.

Parker, S.R., Gammons, C.H., Poulson, S.R., DeGrandpre, M.D., 2007. Diel changes in pH, dissolved oxygen, nutrients, trace elements, and the isotopic composition of dissolved inorganic carbon in the upper Clark Fork River, Montana, USA. *Applied Geochemistry* 22(7): 1329-1343.

Parker, S.R., Poulson, S.R., Smith, M.G., Weyer, C.L., Bates, K.M., 2010. Temporal variability in the concentration and stable isotope composition of dissolved inorganic and organic carbon in two Montana, USA, rivers. *Aquatic Geochemistry* 16: 61-84.

Pawellek, F., Veizer, J., 1994. Carbon cycle in the upper Danube and its tributaries: $\delta^{13}C_{DIC}$ constraints. *Israel Journal of Earth Sciences* 43: 187-194.

Pawellek, F., Frauenstein, F., Veizer, K., 2002. Hydrochemistry and isotope geochemistry of the upper Danube River. *Geochemica et Cosmochemica Acta* 66: 3839-3853.

Phillips, D.L., Jillian, W.G., 2003. Source partitioning using stable isotopes: coping with too many sources. *Oecologia* 136: 261-269.

Pogue, T.R., Anderson, C.W., 1994. *Processes controlling dissolved oxygen and pH in the upper Willamette River Basin*. Washington, D.C: US Geological Survey-Water Resources Investigation Report 95-4205, online at: http://pubs.er.usgs.gov/publication/wri954205.

Post, W.M., Peng, T.H., Emanuel, W.R., King, A.W., Dale, V.H., DeAngelis, D.L., 1990. The Global Carbon Cycle. *American Scientist* 78: 310-326.

Quinlan, J.F., Smart, P.L., Schindel, G.M., Alexander, E.C., Edwards, A.J., Smith, A.R., 1991. Recommended Administrative/Regulatory Definition of Karst Aquifer, Principles for classification of Carbonate Aquifers, Practical Evaluation of Vulnerability of Karst Aquifers, and Determination of Optimum Sampling Frequency at Springs. Dublin, OH: National Ground Water Association, 573-635.

Randerson, J.T., Thompson, M.V., Conway, T.J., Fung, I.Y., Field, C.B., 1997. The Contribution of Terrestrial Sources and Sink to Trends in the Seasonal Cycle of Atmospheric Carbon Dioxide. *Global Biogeochemical Cycles* 11: 535-560.

Raymond, P.A., Cole, J.J., 2003. Increase in the Export of Alkalinity from North America's Largest River. *Science* 301: 88-91.

Redfield, A.C., 1958. The Biological Control of Chemical factors in the Environment. *American Scientist* 46: 205-221.

Rhode, H., 1990. A comparison of the contribution of various gases to the greenhouse effect. *Science* 248: 1217-1219

Scheffer, M., Brovkin, V., Cox, P.M., 2006. Positive feedback between global warming and atmospheric CO_2 concentration inferred from past climate change. *Geophysical Research Letters* 33(10): DOI: 10.1029/2005GL025044.

Schwartz, D., Mariotti, A., Lanfranchi, R., Guillet, B., 1986. $^{13}C/^{12}C$ ratios of soil organic matter as indicators of ecosystem change in the Congo. *Geoderma* 39: 97-103.

Schulte, P., Geldern, R.V., Freitag, H., Karim, A., Negrel, P., Petelet-Giraud, E., Probst, A., Probst, J., Tellmer, K., Veizer, J., Barth, J.A.C., 2011. Applications of stable water and carbon isotopes in watershed research: Weathering carbon cycling and water balances. *Earth Science Reviews* 109: 20-31.

Spiro, B., Pentecost, A., 1991. One Day in the Life of a Stream, a Diurnal Inorganic Carbon Mass Balance for a Travertine-Depositing Stream. *Geomicrobiology* 9(1): 1-11.

Striegl, R.G., Dornblaser, M.M., McDonald, C.P., Rover, J.R., Stets, E.G., 2012. Carbon dioxide and methane emissions from the Yukon River system. *Global Biogeochemical Cycles* 26(4): DOI: 10.1029/2012GB004306.

Szramek, K., Walter, L.M., 2004. Impact of carbonate precipitation on riverine inorganic carbon mass transport from a mid-continent, forested watershed. *Aquatic Geochemistry* 10: 99-137.

Tellmer, K., Veizer, J., 1999. Carbon fluxes, pCO_2, and substrate wreathing in a large northern river basin, Canada: carbon isotope perspectives. *Chemical Geology* 159: 61-86.

Tobias, C., Böhlke, J.K., 2011. Biological and geochemical controls on diel dissolved inorganic carbon cycling in a low-order agricultural stream: Implications for reach scales. *Chemical Geology* 283: 18-30

Urey, H., 1947. The thermodynamic properties of isotopic substances. *Journal of the Chemical Society* 1947*:* 562-571

Urey, H., 1948. Oxygen isotopes in nature and in the laboratory. *Science* 108 (2810): 489-496.

USACE (United States Army Corp of Engineers-Louisville District), 2011. *Green River watershed section 729 initial watershed assessment*. Washington, D.C.: USACE.

USDOE (United States Department of Energy), 2008. *The Carbon Cycle*. Washington, D.C.: Office of Science. Available online: http://genomicscience.energy.gov/carboncycle/index.shtml

USGS (United States Geological Survey-National Water Information System), 2013. *National Water Data*. Washington, D.C.: USGS. Available online: http://waterdata.usgs.gov/nwis (Accessed April 3, 2013).

Waldron, S., Flowers, H., Arlaud, C., McFarlane, S., 2009. The significance of organic carbon and nutrient export from peatland-dominated landscapes subject to disturbance, a stoichiometric perspective. *Biogeosciences* 6: 363-374.

White, W.B., 1988. *Geomorphology and Hydrology of Karst Terrains*. New York, NY: Oxford University Press.

White,W.B., White, E.L., 1989. *Karst Hydrology: Concepts from the Mammoth Cave Area*. New York, NY: Van Nostrand Reinholm.

Wigley, T.M.L., Richels, R., Edmonds, J.A., 1996. Economic and environmental choices in the stabilization of atmospheric CO_2 concentrations. *Science* 379: 240-243.

Wooten, R.D., Tsokos, C.P. 2010. Parametric analysis of carbon dioxide in the atmosphere. *Journal of Applied Sciences* 10: 440-450.

Yang, C., Tlemer, K., Veizer, J., 1996. Chemical dynamics of the "St. Lawrence" riverine system: δH_2O, $\delta^{18}O$-H_2O, $\delta^{13}C$-DIC, $\delta^{34}S_{sulfate}$, and dissolved $^{87}Sr/^{86}Sr$. *Geochimica et Cosmophemimica Acta* 60: 851-866.

Yu, Y., Liu, C., Wang, F., Wang, B., Li, J., Li, S., 2008. Dissolved inorganic carbon and its isotopic differentiation in cascade reservoirs in the Wujiang drainage basin. *Chinese Science Bulletin* 53: 3371-3378.

Zeebe, R.W., Wolf-Gladrow, D., 2001. *CO_2 in Seawater: Equilibrium, Kinetics, Isotopes*. Amsterdam, Netherlands: Elsevier Oceanography Series 65.

Zhang, J., Quay, P.D., Wilbur, D.O., 1995. Carbon isotope fractionation during gas-water exchange and dissolution of CO_2. *Geochimica et Cosmochemica Acta* 59: 107-114.